[Frontiers in Bioscience 9, 3486-3509, September 1, 2004]

DEVELOPMENT OF NEW ANTI-CANCER PEPTIDES FROM CONFORMATIONAL ENERGY ANALYSIS OF THE ONCOGENIC *ras*-P21 PROTEIN AND ITS COMPLEXES WITH TARGET PROTEINS

Matthew R. Pincus [1, 2]

[1] *Department of Pathology and Laboratory Medicine, New York Harbor VA Medical Center, 800 Poly Place, Brooklyn, NY 1209,*
[2] *Department of Pathology, SUNY Downstate Medical Center, 450 Clarkson Avenue, Brooklyn, NY 11203*

TABLE OF CONTENTS

1. ABSTRACT

We have employed a computational approach to design peptides, from known oncogenic proteins, that inhibit tumor growth. This approach has been applied to the *ras*-p21 protein that becomes oncogenic when single amino acid substitutions occur at critical positions in its polypeptide chain, such as at Gly 12 and Gln 61. In this

approach, using two sampling methods, molecular dynamics and the electrostatically driven Monte Carlo (EDMC) method, we have computed the average structures of wild-type and oncogenic forms of *ras*-p21 alone and bound to a number of its target proteins, such as the *ras*-binding domain (RBD) of *raf*, guanine nucleotide exchange protein (GAP) and SOS guanine nucleotide exchange protein (GAP). By superimposing the average structures of the oncogenic forms on those of their wild-type counterparts, we have identified a number of domains that change conformation. These domains are potential effector domains that are involved uniquely in oncogenic *ras*-p21 signaling. We have therefore synthesized peptides corresponding to these domains and tested them in *Xenopus laevis* oocytes for their abilities to inhibit oncogenic *ras*-p21 selectively. Using this approach, we have identified three peptides from *ras*-p21 and one peptide each from the RBD of *raf*, GAP and SOS that selectively inhibit oncogenic but not insulin-activated wild-type *ras*-p21-induced oocyte maturation. We have synthesized the *ras*-p21 peptides attached to a penetratin leader sequence to enable cell membrane penetration and introduced these peptides into a *ras*-transformed pancreatic cancer cell line; these peptides, but not an unrelated negative control peptide, cause the cells to undergo complete phenotypic reversion. On the other hand, none of these peptides has any effect on the growth of untransformed pancreatic acinar cells in culture, further suggesting that they may not interfere with normal cell growth. Thus these peptides can be useful agents in the treatment of cancers. We have further used these peptides to demonstrate that oncogenic and wild-type *ras*-p21 proteins utilize different signal transduction pathways and to identify where these differences occur in cells.

2. INTRODUCTION

While, for many years, oncogenes were known to be major causes of cancers in animals, it is only recently that they have been found to be major, if not exclusive, causes of cancer in humans. These genes are the mutated counterparts of wild-type genes, all of which encode proteins that are involved in the control of mitosis (1). These mutated genes can be introduced into cells by a variety of retro-viruses or through mutations in the endogenous genes through chemical or physical (e.g., x-rays) carcinogenesis.

2.1. Mutated proteins can induce malignant transformation

Mutations in these critical genes generally result in the encoding of proteins that contain amino acid deletions or substitutions at critical positions in their amino acid sequences (1). It is these proteins that then function abnormally and promote uncontrolled cell division. Less commonly, mutations in control regions of the gene can result in overexpression of the protein, resulting in hyperactivation of mitotic processes. Generally, gene deletions result in the encoding of proteins that lack functioning regulatory domains thereby causing them to be constitutively activated.

Most commonly, inappropriately functioning mitogenic proteins result form single amino acid substitutions (1). As discussed in the next section, often almost any one of the naturally occurring amino acids can substitute for the wild-type amino acid resulting in abnormal protein function. This observation suggests the possibility that the arbitrary amino acid substitutions induce changes in the three-dimensional structure of the protein resulting in its permanent activation.

Conversely, there are numerous proteins. such as the p53 protein, that function as anti-oncogenic proteins, i.e., when activated, they block mitosis (2). These proteins block transcription of mRNA encoding mitogenic proteins and induce transcription of mRNA encoding proteins that induce cell cycle arrest and promote apoptosis (2). In contrast to oncogenic proteins, amino acid substitutions in anti-oncogenic proteins cause their permanent inactivation. This results in their inability to block mitosis appropriately. Since, again, arbitrary amino acid substitutions in these proteins inactivate them, it suggests that these substitutions induce important structural changes in these proteins, inactivating them.

Importantly, whenever these amino acid substitutions at critical positions in the amino acid sequences occur either in an oncogene or in an anti-oncogene protein, they become phenotypically dominant, despite the fact that the cell is often heterozygous for the protein. Thus, for example, substituted oncoproteins induce uncontrolled cell division despite the fact that the wild-type protein is also present at a similar intracellular concentration.

2.2. Mutant *ras*-p21 protein is a major cause of cancer

A critically important oncogene, and the first one to be discovered as a cause of a human tumor, a bladder carcinoma, is the *ras* gene, that was known to induce *ra*t *s*arcomas (hence the name, *ras*). When the *ras* gene from the human bladder cancer, but not the *ras* gene from normal cells, was transfected into quiescent mammalian NIH 3T3 cells, it induced cell transformation, i.e., the cells underwent uncontrolled proliferation, became "heaped up" on one another, became aneuploid and formed metastatic tumors when explanted into nude mice (3).

Sequencing of both genes, from transformed and normal cells, revealed that the only difference between them was a single base change in the twelfth codon of the first exon in which a GGC was replace with GTC. This results in the substitution of a Val residue for the normally occurring Gly residue at position 12 in the amino acid sequence of the *ras*-gene-encoded protein (3).

The *ras*-gene-encoded protein has 189 amino acids and an Mr of 21 kD and is called the *ras*-p21 protein. Both wild-type and Val 12-substituted *ras*-p21 have been bacterially over-expressed and micro-injected into NIH 3T3 cells. Val 12-p21, but not its wild-type counterpart protein, induces cell transformation of this cell line, showing that it is the mutated *ras*-p21 protein that is the actual transforming agent (3, 4). At present, it has been found that oncogenic forms of *ras*-p21 occur in about one out of every three common human tumors,

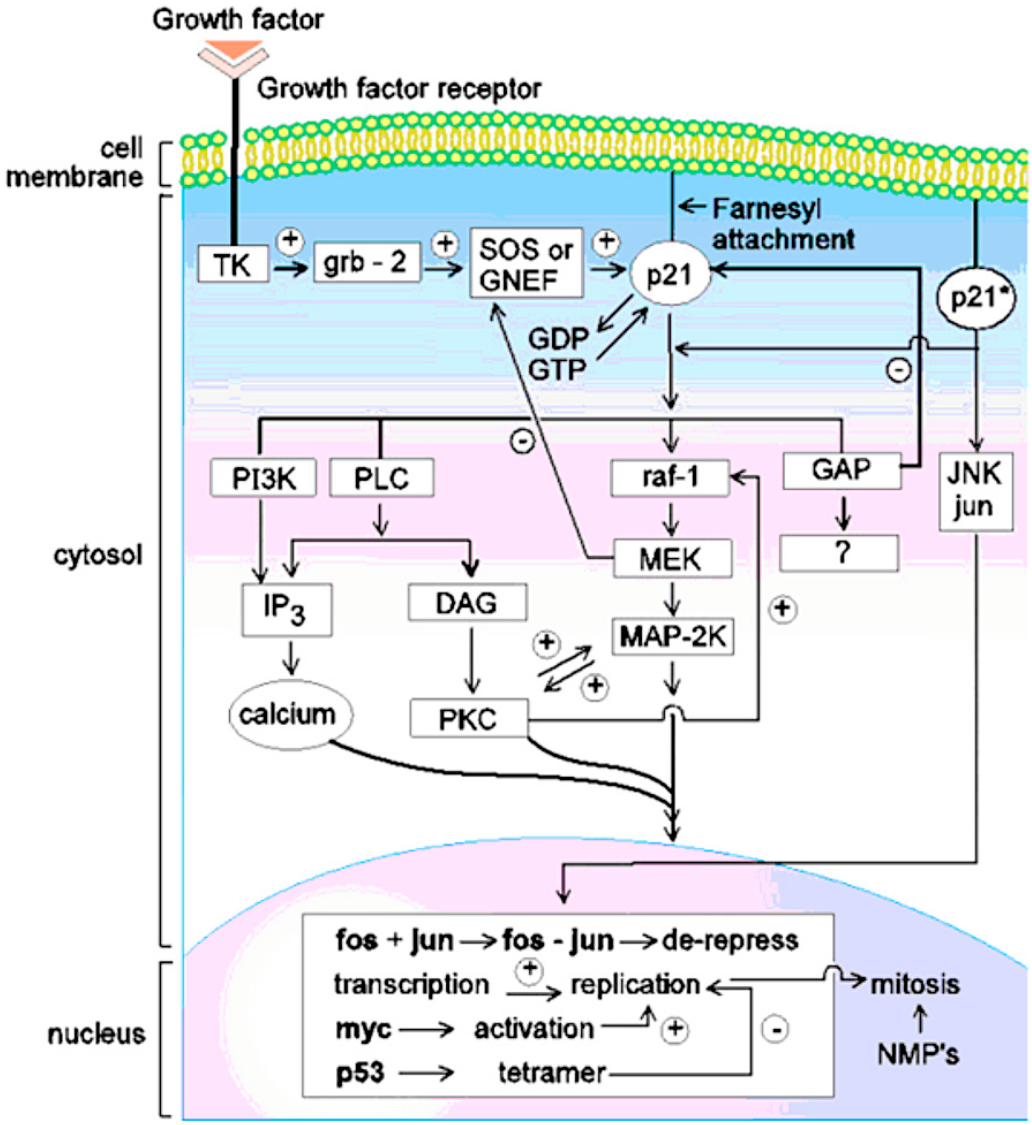

Figure 1. Overall events on the *ras* signal transduction pathway, beginning (top, left) when a growth factor binds to its cell receptor. This results in activation of intracytoplasmic tyrosine kinase (TK) activity on the receptor that binds to the adapter grb-2 protein that concurrently binds to and activates the guanine nucleotide exchange factor (GNEF), SOS. This, in turn, induces *ras*-p21 to exchange GDP for GTP, resulting in its activation. *ras*-p21 is bound to the inner cell membrane by a covalent farnesyl moiety attachment in thioether linkage to Cys 186. In its GTP-bound form *ras*-p21 binds to a number of other target proteins. One of these is GAP (GTPase a7ctivating protein) that induces GTPase activity in *ras*-p21 resulting in hydrolysis of GTP to GDP cycling *ras*-p21 into the inactive state (minus sign on arrow from GAP box). However, as discussed in the text, GAP may also be involved as a target in *ras* signaling, hence the question mark below the GAP box. Activated *ras*-p21 also binds to and activates *raf* (shown in the upper middle of the figure), a 74 kDa Ser/Thr kinase protein that, in turn, activates the kinase cascade in which it activates MEK that finally activates ERK (MAP-2K in the figure). This protein shuttles between the cytosol, where it is involved in cytoskeletal rearrangements, and nucleus in which it activates a critically important nuclear transcription factor, *fos* that forms a heterodimeric complex with another critically important nuclear transcription factor, *jun*. The latter protein is activated by another kinase, *jun*-N-terminal kinase (JNK), that occurs on a separate pathway called the stress-activated protein (SAP) pathway. As explained in the text, oncogenic *ras*-p21 directly activates JNK/*jun* that circumvents the normal, regulated wild-type *ras*-p21-activated pathways (right side of the figure). *ras*-p21 also interacts directly with phosphoinositol-3-hydroxy kinase (PI3K, left side of the figure) and induces activation of phospholipase C (PLC); both of these proteins cause increases in the second messenger molecule, inositol triphosphate (IP_3) and diacylglycerol (DAG); the former induces calcium mobilization while the latter induces activation of protein kinase C (PKC) that is especially critical to the oncogenic *ras*-p21 pathway. In the nucleus, the *fos-jun* complex, also called AP1, induces transcription of many pro-mitogenic proteins including cyclins and possibly the nuclear skeletal proteins called nuclear matrix proteins (NMP's); other nuclear proteins, like *myc*, also transcriptionally active, are also often activated in this process. Anti-oncogene proteins, such as p53, also become activated. This protein blocks transcription of pro-mitotic proteins (minus sign on p53 arrow) and induces apoptosis in transformed cells.

including over 90 percent of pancreatic cancers and in at least 50 percent of colon cancers (1).

Oncogenic, but not wild-type, *ras*-p21 induces maturation (completion of meiosis) of *Xenopus laevis* stage VI, metaphase-arrested oocytes in the second meiotic division (5). Importantly, these oocytes express insulin receptors; insulin induces oocyte maturation and requires activation of endogenous normal cellular *ras*-p21 in this process (6). Thus oocytes are of great value in discriminating between agents that affect oncogenic vs wild-type *ras*-p21 (7).

In addition, oocytes contain progesterone receptors. Progesterone induces oocyte maturation by *ras*-independent pathways (6). This agent is therefore useful in testing for specificity of agents that inhibit both oncogenic and activated endogenous wild-type *ras*-p21 for their specificity for the *ras* pathway.

As summarized in Figure 1, to be active, *ras*-p21 protein must be bound to the cell membrane via its Cys 186 linked as a thioether to a farnesyl moiety promoted by a farnesyl transferase (8). To induce mitosis, therefore, it must induce other proteins to become activated in a chain that ends in the nucleus, in a mitogenic signal transduction pathway.

2.3. *ras*-Induced signal transduction pathways

Much is now known about the upstream components of the normal *ras*-p21 signal transduction pathway. First, *ras*-p21 is known to function as a G-protein,that is, it is activated by binding GTP in place of the normally bound GDP. This exchange is promoted by the binding of a growth factor to its transmembrane receptor, resulting usually in receptor dimerization. This results in activation of a tyrosine kinase that is part of the intracytoplasmic domain of the growth factor receptor (reviewed in ref. 1).

In its activated state, as shown in Figure 1, the tyrosine kinase binds to an adapter protein called grb-2 that concurrently binds to a vitally important protein called SOS that is a guanine nucleotide exchange promoter protein. Activation of SOS results in its binding to *ras*-p21, promoting the exchange of GDP for GTP and activation of the latter protein (reviewed in ref. 1).

Opposing this process, the protein GTPase activating protein or GAP, also binds to *ras*-p21 such that it enhances endogenous *ras*-p21 GTPase activity, resulting in its hydrolysing GTP back to GDP (Figure 1). Thus SOS and GAP are thought to control the levels of activated *ras*-p21 at any time intracellularly (1).

Once activated, p21 activates a number of critical proteins such as phospholipase C-gamma and phosphoinositol-3-hydroxy kinase (PI3K) both of which activate a number of vital second messenger molecules such as diacylglycerol that activates protein kinase C (PKC), critically important for oncogenic p21 action, and inositol triphosphate (IP_3). Besides PI3K, *ras*-p21 interacts directly with a number of target proteins, one of the most important of which is the *raf*-p74 protein (1).

This protein becomes activated when it binds to *ras*-p21 in the cell membrane and, in turn, activates a set of phospho kinase cascade reactions. In this cascade, activated *raf*-p74 directly activates mitogen (extracellular) kinase or MEK that, in turn, activates mitogen-activated protein kinase (MAPK) or extracellular mitogen response kinase (ERK). This protein is vital; it promotes cytoskeletal rearrangements for mitosis and shuttles between the cytosol and nucleus, where it activates the all-important protein, *fos* which forms a hetero-dimeric complex with another protein, *jun*. This complex strongly promotes transcription of mitosis-promoting proteins (1).

jun protein is activated by another kinase system, i.e., the stress-activated protein (SAP) kinase proteins. Its immediate activator is *jun*-N-terminal kinase (JNK) (9). As shown in Figure 1, direct activation of *jun* may be effected by oncogenic *ras*-p21 (p21 in the figure). As also shown in this figure, other cooperative proliferation signals may originate from other oncoproteins such as nuclear *myc* while, concurrently, anti-proliferation signals may be generated from the activated nuclear p53 anti-oncogene protein. As shown on the right side of Figure 1, and as we discuss further below, oncogenic *ras*-p21 can interact directly with JNK/*jun*, bypassing the normal, regulated pathways and can thereby induce uncontrolled cell proliferation (1).

2.4. Direct interactions between *ras*-p21 and target proteins depends largely on two of its domains

In the above sequence of events, *ras*-p21 interacts directly with at least four intracellular proteins, viz, *raf*, GAP, SOS and PI3K. Surprisingly, it uses the same switch 1 domain involving residues 32-47, consisting of an exposed beta-sheet, in binding to all four of these proteins (10-13). Yet, there are no consensus sequences in these four proteins for binding to this *ras*-p21 domain, and, indeed, in the x-ray structures for *ras*-p21 bound to these proteins, there are substantially different interactions between the switch 1 domain and the binding determinants for each complex (10-13).

In addition, another domain, called the switch 2 domain, involving residues 55-71, is vital in the interaction of *ras*-p21 with GAP and SOS proteins (11, 12). This domain contains Gln 61, a critical residue (see above), that has been implicated in interacting with wild-type Gly 12 and in promoting GTP hydrolysis cooperatively with the backbone NH of Gly 12 (14). Despite its functional importance, the switch 2 domain is not well-defined structurally except in *ras*-p21 complexes with SOS with which it has many interactions and, to a lesser extent, with GAP (11-14).

Besides interacting with nucleotide, specific residues from switch 1 and 2 domains interact with a magnesium ion that interacts with the terminal phosphate residue of GTP (14). Two important residues that lie close to the magnesium ion are Ser 17 of the switch 1 domain and the backbone NH atoms of Ala 59 of the switch 2 domain. These two residues, together with other amino acid residues from these two domains, are thought to be involved in chelation of this ion.

2.5. How amino acid substitutions in *ras*-p21 can induce it to become oncogenic

Importantly, *ras*-p21 proteins that contain any

amino acid except for Pro, that substitutes for Gly 12, all induce cell transformation (reviewed in ref. 7). Similar results have also been obtained for *ras*-p21 proteins with arbitrary amino acid substitutions for Gln 61 and Gly 13 (15). These observations suggest that amino acid substitutions for these critical amino acid residues might induce the protein to change conformation allowing it to remain activated for prolonged times.

Alternatively, it has been found that substitutions of amino acids for Gly 12 and for Gln 61 cause large rate reductions in GAP-induced hydrolysis of GTP. This can result in prolonged activation of *ras*-p21 (11, 14). In the structure of wild-type *ras*-p21 bound to GTP analogues, the backbone NH of Gly 12 and the carboxamido NH of Gln 61 appear to interact with the beta-gamma bridging oxygen of the gamma-phosphate residue and are thought to aid in the departure of the terminal phosphate leaving group (14). In complexes of substituted *ras*-p21 proteins complexed with GTP analogues, this alignment is disrupted, suggesting a mechanism for prolonged *ras*-p21 activation (11, 14).

However, the latter cannot explain the effects of a number of substitutions on p21 activity. Thus, substitution of Pro for Gly 12 is the only non-oncogenic substitution that occurs at this position (3). Yet Pro 12 has no NH backbone atom that can contribute to GTP hydrolysis. On the other hand, substitution of Gly for Gln 61 is oncogenic but the rate of GTP hydrolysis of this substituted protein is not decreased (15). Other mutated p21 proteins, such as one containing a D38E (a Glu-for-Asp substitution), bind strongly to GTP and to GAP, do not undergo hydrolysis, and yet do not transform cells (14).

Very importantly, a triply-substituted p21 protein with Val for Gly 10, Arg for Gly 12, and Thr for Ala 59 has been found to cause cell transformation, but this protein does not bind either GDP or GTP (16). On the other hand, a similar protein with Arg for Gly 12, Val for Gly 15 and Thr for Ala 59 neither transforms cells nor binds nucleotide (16). Here, since these proteins do not interact with nucleotides, differences in the rates of hydrolysis of GTP cannot explain the differences in activities of these two proteins. Thus it is plausible that the different activities of these two proteins are caused by structural differences between them.

Finally, when it was discovered that activated *ras*-p21 binds directly to *raf*, it was found that, while wild-type *ras*-p21 bound to GDP did not bind to *raf,* Val 12-*ras*-p21 bound to GDP could bind to a significant extent to this critical protein (17). This suggests that the G12V substitution induces a significant change in the structure of *ras*-p21 that enables it to interact with intracellular targets even without binding to GTP.

In this paper, we present evidence that single (or, in some cases, several) amino acid substitutions at critical positions in the linear amino acid sequence of the *ras*-p21 protein induce important conformational changes in protein domains that are critical to the process of mitogenic signal transduction. We have employed the methods of conformational analysis to determine which regions of these proteins undergo conformational changes in response to these substitutions.

We have then synthesized peptides corresponding to these domains and assayed them for their abilities to block oocyte maturation induced either by oncogenic *ras*-p21 or by insulin that requires activation of wild-type *ras*-p21. Using this procedure, we have identified several *ras*-p21 peptides that selectively block oncogenic *ras*-p21 and block the growth of mammalian cancers by inducing them to revert to phenotypically untransformed cells. These same peptides do not affect normal cell growth, however, suggesting that they selectively affect cancer cells.

Since the x-ray structures of *ras*-p21 bound to many of its target proteins, in particular *raf* (the *ras*-binding domain), SOS and GAP, have been solved, we extend our analysis to these complexes. This analysis has allowed us to detect domains in these target proteins that change conformation when oncogenic *ras*-p21 is bound to them compared with their structures when they are bound to wild-type *ras*-p21. We have further identified peptides from these target proteins that selectively block oncogenic *ras*-p21. Like the *ras*-p21 peptides, these latter domain peptides may be effective in the treatment of *ras*-induced human cancers.

3. METHODS

3.1. Computational methods

3.1.1. Basic aim

The overall goal of our computational approach is to compute the lowest energy structures available to wild-type and oncogenic *ras*-p21 alone and in complexes with its target proteins, using their x-ray structures as the starting points. Once the low energy structures are computed, they are used to compute an average structure (discussed in the next section). The average structures are then superimposed to determine which domains differ in conformation between oncogenic and wild-type proteins alone and in their complexes.

3.1.2. Overall methodology

All computational methods are based on the assumption that the energy-minimized x-ray crystal structure of a protein is the lowest energy (global) minimum conformation for the given amino acid sequence (18). This structure occurs in a potential energy well in which other low energy conformations of the protein exist which have the same basic chain fold but which differ in conformation from the energy-minimized x-ray structure locally. The observed structure in solution is then an average of these low energy structures that occur in the global energy minimum potential well for each protein (7, 18). Determination of these low energy structures requires the use of sampling methods. We have employed two types.

1. *Molecular dynamics* samples these alternate conformations by integrating, with respect to time, Newton's equations of motion, i.e., the force on the molecule is the negative of the first derivative of the potential function with respect to the coordinates of each of the atoms. The energy-minimized starting structure is first subjected to a procedure in which it is heated from 0^{o}K to 300^{o}K in increments of 5^{o}K. At each temperature, molecular dynamics trajectories are computed for 50 fsec in which velocities are assigned randomly to each atom from a Maxwellian distribution of molecular velocities, characteristic of the particular temperature. After heating to

300°K, the structure is then allowed to equilibrate for an additional 50 psec so that the computed average temperature for the complex is 300°K.

The dynamics trajectory for the system is then followed for 2 nsec. In all of the computations, integrations for the trajectories are performed over 1 fsec intervals using the Verlet integration algorithm. The total times over which the integration occurs are generally in the nsec range. On the resulting trajectory, the low energy structures around the starting structure are computed (19).

For each protein structure or complex, we find that the trajectories that are computed over this time interval are such that the total energy converges to a low, constant value. The structures whose energies have converged are then used to compute the average structure.

In these calculations, we have employed two sets of potential functions in these computations, AMBER and DISCOVER (20, 21). With both sets of potential functions, we have used two types of solvation models: one, in which a distance-dependent dielectric constant is used and the other in which explicit water molecules are included over a cubic grid using periodic boundary conditions.

2. The *Electrostatically-Driven Monte Carlo EDMC Method* (22, 23), based on ECEPP potential functions (24) samples conformations of the protein in the global minimum potential by perturbing the energy-minimized x-ray structure by determining the electric field of the local energy minimum. The dipole moments of the backbone CO-NH groups are then examined to determine which dipole or group of dipoles is (are) the least optimally oriented with the field. The dihedral angles of these peptide groups are then changed to orient these dipoles to become aligned with the field, and the energy of the resulting structure is minimized again. This procedure is repeated iteratively until the energy of the protein is lowered no further. This method is referred as the self-consistent electric field (SCEF) (22) method and has been extended so that at the end of a set of self-consistent calculations, the structure is randomly perturbed using the Monte Carlo method (23), and the process described above is repeated. In this manner, sets of low energy structures are generated for the given starting structure. The average structure of each protein is then computed as the Boltzmann average of all of the low energy structures computed on the energy minimization "trajectory".

Once the low energy structures have been sampled, coordinate fluctuations for each residue of the protein are computed as the average root mean square (rms) deviations of the coordinates of the atoms of each residue for each contributing structure from those of the average structure. Superimposition of average structures for two different forms of *ras*-p21 and *ras*-p21 complexed with a target protein is performed such that the root mean square (rms) deviation of the backbone atoms of the two structures is a minimum. In this manner, comparison of the average structures for normal and oncogenic forms allows identification of regions that differ in their three-dimensional structures.

3.1.3. Proteins studied

We have applied our computational approach to wild-type and oncogenic forms (Val 12- and Leu 61-substituted) of *ras*-p21 bound to GDP and GTP. In addition, we have studied two triply-substituted forms of *ras*-p21, neither of which bind nucleotide at all: the first is (G12R, G15V, A59T)-p21 and the second is (G10V, G12R, A59T)-p21. The first of these is non-transforming while the second one is strongly transforming (16). Comparison of the average structures for these proteins has revealed the specific conformational changes that occur in the oncogenic form of the protein since nucleotide binding is not a factor for consideration in the activity of these two proteins.

We have also extended our analysis to comparing the average structures of wild-type and Val 12-*ras*-p21 bound to three of its targets: the *ras*-binding domain (RBD) of *raf* (residues 55-131), SOS and GAP. Since we have recently found that glutathione-S-transferase-pi (GST-pi) is a strong and specific inhibitor of the JNK-*jun* system (25, 26), we have also computed its average structure free and bound to an inhibitor, glutathione sulfonate (27), that blocks its ability to affect the JNK-*jun* system.

3.1.4. Generation of starting structures

For wild-type *ras*-p21 alone bound to GDP or GTP, and bound to each of its target proteins, the x-ray structures (14) or computed structures from alpha-carbon tracings of the x-ray structures (28) were subjected to energy minimization. The energy-minimized structures were then directly used for molecular dynamics and EDMC calculations. For the oncogenic forms of *ras*-p21, amino acid substitutions were introduced such that the substituting amino acids were generated using the same set of backbone dihedral angles as for the native Gly residue (29, 30), and the side chain conformations were set in their lowest energy minima for the given backbone minimum (31). The energy of this starting structure was then initially minimized such that only the dihedral angles of Val 12 and its four nearest neighbor residues on both amino and carboxyl terminal ends were allowed to vary. Following this step, the resulting complex was subjected to energy minimization in which all of the atoms of the complex were allowed to move.

3.2. Materials and methods

3.2.1. Proteins

Val 12-Ha-*ras*-p21 and the normal Gly 12-p21 proteins were overexpressed in *E. coli* using the pGH-L9 expression vector containing the chemically synthesized Ha-*ras* gene, as previously described (32). Bovine serum albumin was purchased from Sigma (St. Louis, MO).

3.2.2. Peptides

The following peptides were synthesized by solid phase methods and purified by HPLC to >95 percent purity as revealed by mass spectroscopy (Macromolecular Resources, Colorado State University, Fort Collins, CO): ***ras*-p21 peptides** 35-47 (TIEDSYRKQVVID), 96-110 (YREQIKRVKDSD DVP), 67-77 (MRDQYMRTGEG) and 122-138 (ARTVESRQ AQDLARSYG); ***raf* peptides, from its *ras* binding domain (RBD)**, residues 62-76 (FLPNKQRTVVNVRNGM), 97-110(AVFRLLHEHKGKKA) and 111-121 (RLDWNTDA ASL), 84-92 (negative control, Lys-Ala-Leu-Lys-Val-Arg-Gly-Leu-Gln); **human SOS** sequence 631-641 (YRSFCKPQELL), 676-691 (RFRKEYIQPVQLRVLN), 718-729 (IGTVRGKAM KKW), 994-1004

(LNPMGNSMEKE), 589-601 (EENMQPKAGIPII), 654-675 (EPTEADRIAIENGDQPLSA ELK), 746-761 (NGPGHNITFQSSPPTV), 980-989 (CLRV ESDIKR) and negative control peptide 809-815 (Trp-Thr-Lys-Glu-Asp-Lys-Glu); and **GAP peptides:** 819-827 (LKIMES KQS), 832-845 (PSKLEKNEDVNTNL), 917-926 (IISDSPS PIA), 943-953 (LVEFGAKEPYM) and 1003-1021 (VAHSEL RTLSNERGAQQH). Another negative control peptide was synthesized, the X13 sequence from mammalian cytochrome P450 (MPFSTGKRIMLGE). In addition to these peptides, effector domain peptides from the pi-isozyme of glutathione-S-transferase (GST-pi) were synthesized as follows: residues 34-50 (TIDTWMQGLLKPTCLYG), 99-121 (LRGKYVTLIY TNYENGKNDYVK), 165-182 (LAPGCLDNFPLLSAY VAR), 165-175 (LAPGCLDNFPL), 169-182 (CLDNFPLL SAYVAR) and 194-201 (SSPEHVNR).

Several of these peptides were synthesized with the penetratin leader sequence KKWKMRRNQFWVKVQRG, designated as "leader," on their carboxyl terminal ends, to enable transport across mammalian cell membranes. These include *ras*-p21 peptides 35-47 and 96-110.

3.2.3. c-DNA

The cDNA's for *c-raf*, dominant negative *raf* with a substitution that inactivates its ability to phosphorylate MEK, constitutively activated MEK (caMEK) and *raf* (*raf* BXB, which contains a deletion of residues 27-301 and a Gly-Thr insertion) were prepared as described previously (33, 34).

3.2.4. Plasmids

We have prepared lac-inducible plasmids expressing ampicillin resistance, encoding the two *ras*-p21 peptides 35-37 and 96-110 (33), that were transfected into TUC-3 cells described below. Cells expressing these peptides were selected for on ampicillin-containing media as described previously (33, 35).

3.2.5. Oocyte microinjection

Oocytes were obtained from *Xenopus laevis* frogs from Connecticut Valley Biological (Southhampton, MA) as described previously (34). Microinjected oocytes were incubated in Barth's medium (Specialty Media, Lavellette, NJ) or Barth's medium containing insulin for 36 or 48 hours at 19^{o}C. Oocyte maturation was judged by observing germinal vesicle breakdown (GVBD) (34).

For experiments involving cDNA's, each cDNA was injected at a concentration of 100 micro g/ml; protein expression occurs about 8 hours post-injection (33). The two p21 peptides were microinjected at concentrations of 250 and 500 micro g/ml; the X13 control peptide was injected at a concentration of 500 micro g/ml. Bovine serum albumin was injected at a concentration of 100 micro g/ml.

3.2.6. Cells

As described in several prior publications (35, 36 and references therein), we have developed two cell lines, one a normal contact-inhibited line of rat pancreatic acinar cells, called BMRPA1.430 (BMRPA1) cells and the other a pancreatic acinar carcinoma obtained by transfection of BMRPA1 cells with a plasmid containing an activated human K-*ras* oncogene [single base mutation at codon 12, valine substitution for the wild type glycine in the ras protein (K-ras^{val12}); a kind gift of Dr. M. Perucho (CIBR, La Jolla, CA)] and a neomycin resistance gene. BMRPA1 cells have an epithelial cell phenotype, form acinar structures in culture, have no c-ki-*ras* nor p53 mutations, are unable to grow in anchorage-independent conditions and do not form tumors in Nu/Nu mice (35, 36 and references therein). In addition, they phenotypically maintain differentiated cell functions such as continued enzyme production and activation of zymogen secretion by secretagogue. On the other hand, *ras*-transformed BMRPA1 or TUC-3 cells, selected after transfection for their resistance to G418 and the overexpression of K-ras^{val12}, no longer display an epithelial cell phenotype and acinar cell functions; they grow significantly faster than BMRPA1 cells, have a transformed spindle cell phenotype and form colonies under anchorage-independent conditions *in vitro* and tumors *in vivo* in nude mice.

4. RESULTS AND DISCUSSION

4.1. Conformational analysis of wild-type and oncogenic *ras*-p21

We first analyzed the average structures of the two triply-substituted *ras*-p21 proteins, neither of which binds nucleotide, since mode of binding of GTP cannot be a factor in explaining why one of the proteins (G12R, G15V, A59T)-p21 transforms cells and the other (G10V, G12R, A59T)-p21 does not (37). These studies were performed using the EDMC method (22, 23). Superposition of the two average structures showed that six domains change conformation in the oncogenic protein, viz, residues 10-16 (containing Val 12), the switch 1 35-47 segment, 55-71, the switch 2 segment, 81-93, 96-110 and 115-126 (37). These domains co-incide with domains that were found to have relatively high flexibility in *ras*-p21 bound to GDP (37).

These results raised the question of how the amino acid substitutions in the amino terminal domain of the protein can induce changes in the three dimensional structure of domains that are remote from this region and with which these residues do not directly interact. To answer this question, we studied pairwise correlations between conformational changes in all of these domains. We found that the changes in structure of each domain correlated strongly with changes in structure of the 55-71 domain and much less with the structural changes in any other domain. Thus the switch 2 domain in *ras*-p21 appears to be a conformational switch; induction of changes in conformation of this domain from the amino terminal region induces changes in structure of residues more toward the carboxyl terminal region of the protein.

It would appear that the switch 2 domain of *ras*-p21 is suited to transmit structural changes between different domains in this protein. It has been found to be a highly flexible domain that can therefore function in this capacity.

We then further computed the average structures for several GTP-binding forms of *ras*-p21, including Val 12-p21 and Leu 61-p21 utilizing both EDMC and molecular dynamics approaches. Superposition of the average structures of these two proteins, and wild-type *ras*-p21, bound to GTP on that for the wild-type protein bound to GDP, obtained by either method, are shown in Figure 2 (29, 30, 37). It should be noted that the x-ray structures of *ras*-p21 are for residues 1-166 (14) or 1-171 (38) but not

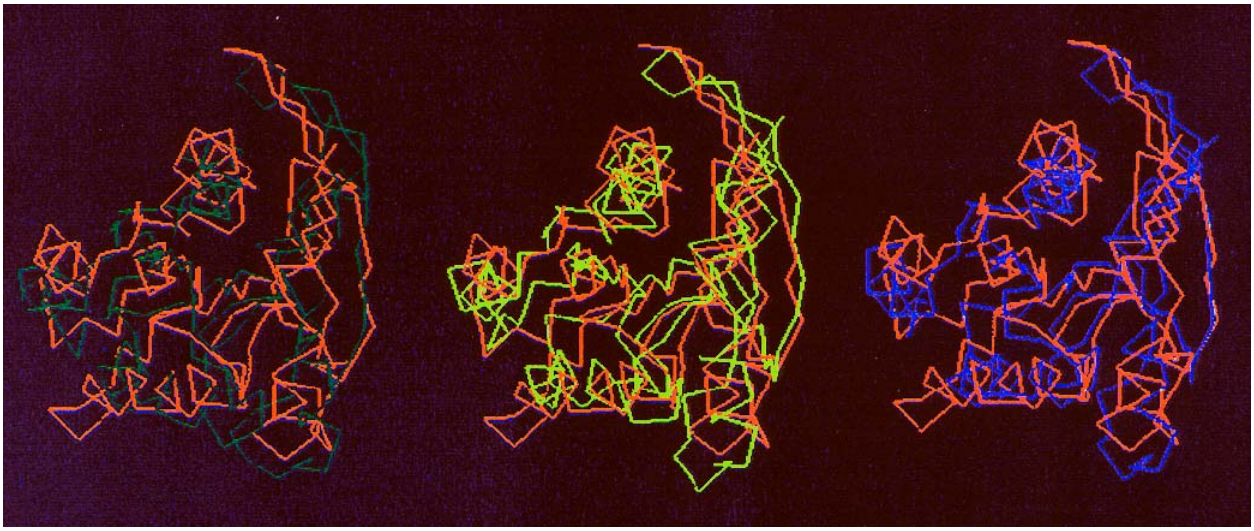

Figure 2. Superposition of the computed average structures, on that for inactive *ras*-p21 bound to GDP (purple structure in each panel), for Val 12-*ras*-p21 (rightmost, blue); wild-type *ras*-p21 bound to GTP (middle panel, yellow); and Leu 61-*ras*-p21 (leftmost panel, green).

for the full-length protein containing 189 amino acid residues since it has not been possible to crystallize the whole protein (14, 38).

However, we have used conformational energy calculations based on ECEPP to compute the low energy structures for the entire carboxyl terminal domain of *ras*-p21 from residues 171-189 and have fused these structures onto the energy-minimized x-ray structure of residues 1-171 of *ras*-p21 and have minimized the energies of these starting structures (39). The lowest energy structures were all found to have the carboxyl terminal segment around Cys 186, linking the protein to the inner cell membrane, close to the amino terminal domain of the protein containing Gly 12. This result suggested the possibility that activation events, such as oncogenic amino acid substitutions at Gly 12, can be linked to membrane events at the carboxyl terminal end of the protein (39).

Importantly, the results shown in Figure 2 are independent of the sampling method (EDMC and molecular dynamics) and the potential functions used. In this figure, the Val 12-(blue, rightmost), activated normal Gly 12-(bound to GTP) (yellow, middle) and Leu 61-(green, leftmost) structures are superimposed on the inactive normal structure (Gly 12-p21 bound to GDP, purple), as the reference in each of the three frames.

From Figure 2, it may be seen that all three structures, blue, yellow and green, deviate locally from the purple structure although the overall three-dimensional structures for all of these proteins is the same. Overall, six domains were found to undergo structural changes in the oncogenic forms, i.e., 10-16, 35-47, 55-71, 81-93, 96-110 and 115-126. Of major note is that the two oncogenic forms (Val 12- and Leu 61-containing) *ras*-p21 proteins undergo strikingly similar conformational changes, indicating that both oncogenic substitutions induce the same changes in structure.

This is seen more clearly in Figure 3 for major segments of *ras*-p21, i.e., 10-16, 35-47, 96-110 and 115-126 (125 in the figure), that undergo significant structural changes, using the same color code as in Figure 2. It can be seen that the Val 12 (blue), activated normal (yellow) and Leu 61-p21 (green) structures cluster together away from that of the inactive wild-type (purple) structure. Also note that the two oncogenic forms of p21 tend to cluster the most with one another, suggesting differences in conformation between the activated wild-type and oncogenic forms of the protein.

4.1.1. Peptides that Block Oncogenic *ras*-p21 Selectively

Based on these results, we synthesized peptides corresponding to each domain of p21 that differed in conformation from that of the wild-type protein. We then injected each of these into oocytes either together with *ras*-p21 or into oocytes which were then incubated with insulin to determine if any of these peptides inhibited oncogenic p21 selectively.

The results are summarized in Figure 4, which includes all of the results that we have obtained from over 40 peptides that we have synthesized that correspond to potential effector domains of *ras*-p21 and of three of its targets, *raf*, SOS and GAP. The top two entries of the figure show the extent of oocyte maturation induced by Val 12-*ras*-p21 and insulin, respectively, in the absence of any potential effector domain peptides. All of the remaining entries are paired and show the effects of each putative effector domain peptide, that we have identified by our computational approaches, on Val 12-*ras*-p21- and insulin-induced oocyte maturation, respectively. The effects of several control peptides are also shown (entries 45 and 46 and 47 and 48) for the negative control X-13 and a domain peptide from the *ras*-binding domain of *raf* that does not undergo conformational changes when bound to oncogenic

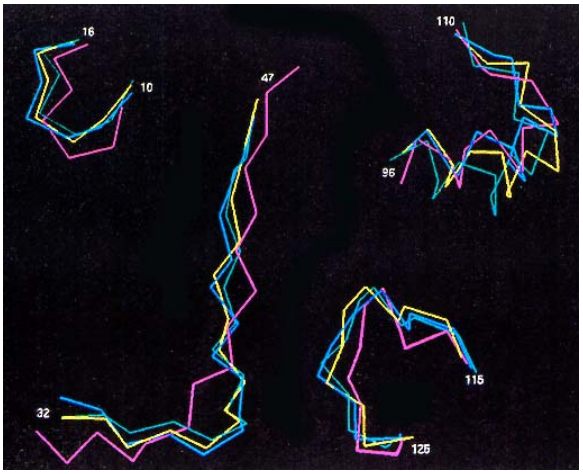

Figure 3. Conformations for four *ras*-p21 domains, residues 10-16, 32-47, 96-110 and 115-125, from the superpositions in Figure 2, that undergo significant changes in structure in oncogenic and activated *ras*-p21. The color scheme is the same as for Figure 2.

ras-p21 as discussed in Section 4.2.3 below. Other control peptides and proteins such as a peptide from the CD4 receptor protein, angiotensin, bovine serum albumin all were found to have no effect on Val 12-p21- and insulin-induced oocyte maturation (not shown). As can be seen in Figure 4, *ras*-p21 peptides 35-47 (entries 3 and 4), 96-110 (entries 7 and 8) and 115-126 (entries 9 and 10) all have a much more pronounced inhibitory effect on oncogenic (Val 12-)*ras*-p21-induced maturation than on insulin-induced maturation. Since all three peptides selectively block oncogenic p21 but only minimally affect activated normal p21, these peptides are excellent candidates for blocking oncogenic *ras*-p21-induced tumors but not normal cell growth.

4.1.2. Peptides that Selectively Block Oncogenic *ras*-p21 in Oocytes Block Tumor Cell Growth

To confirm the above hypothesis, we have tested these peptides for their abilities to block the growth of *ras*-induced tumor cells (35). For these experiments we have utilized two cell lines that we have developed in our laboratory, one a normal rat pancreatic acinar cell line (called BMRPA1) and the other a Val 12-*ras*-p21-induced counterpart pancreatic cancer cell line, called TUC-3, produced by stable transfection of the K-*ras* oncogene into the BMRPA1 cell line (34, 35).

We introduced each peptide into the cells in two ways: in the first, each peptide was synthesized attached on its carboxyl terminal end to the penetratin or leader sequence that enables peptides and proteins to cross cell membranes (33, 35). In the second, we transfected lac-inducible plasmids that encode each of the peptide sequences into TUC-3 cells (33, 35).

A typical result, using the *ras*-p21 96-110-Leader peptide, is shown in Figure 5 (35). Panel A shows untreated, untransformed BMRPA1 cells while Panel B shows that treatment of these cells with the *ras*-p21 96-110 peptide has no effect on cell viability (or growth, not shown). In contrast, Panel C shows untreated TUC-3 pancreatic cancer cells that, when treated for two weeks with *ras*-p21-Leader peptide, at doses as low as 1 micro g/ml, undergo complete reversion to the untransformed phenotype as shown in Panel D. On the other hand, the negative control X13-Leader peptide had no effect on the growth of either TUC-3 or BMRPA1 cells suggesting specificity of the 96-110-Leader peptide (results shown in ref.35).

We obtained identical results on TUC-3 cells that were transfected with plasmids encoding the *ras*-p21 35-47 and 96-110 sequences and selected on G418 media. In contrast, TUC-3 cells transfected with the Lac-inducible plasmid encoding the X13 sequence did not undergo phenotypic reversion (35).

To test definitively that the *ras*-p21 96-110-Leader peptide-treated TUC-3 cells really undergo phenotypic reversion, we explanted these apparently revertant cells into the peritoneal cavities of nude mice. There was no cell growth found over an observation period of two months while X13-Leader-treated cells grew rapidly such that metastatic tumors occurred in less than five weeks, verifying that the *ras*-p21 peptide-treated cells were truly phenotypically revertant (35).

Given our findings that the *ras*-p21 35-47-Leader and 96-110-Leader peptides, but not the X-13-Leader control, induce TUC-3 cell phenotypic reversion and that none of these three peptides have any effect on the growth of BMRPA1 cells, we conclude that the two *ras* peptides are specific for transformed cells. Furthermore, the fact that TUC-3 cells underwent identical phenotypic reversion when transfected with the lac-inducible plasmids encoding either *ras*-p21 sequence but not with the X13 sequence (35) suggests that the *ras* peptide itself induces phenotypic reversion independently of the presence of the leader (penetratin) sequence.

It should be noted that identification of these domain peptides resulted directly from the conformational energy analysis. Since the *ras* peptides affect oncogenic *ras*-p21 as opposed to its wild-type counterpart protein and since they block tumor cell growth without affecting normal cell growth, it appears that oncogenic and wild-type *ras*-p21 utilize different signal transduction pathways. We have been investigating where these pathways diverge from one another.

4.1.3. Oncogenic and Activated Normal *ras*-p21 Proteins Utilize Divergent Signal Transduction Pathways

In former studies, we have found that azatyrosine (AzTyr), which is known to have a powerful anti-proliferative effect on *ras*-transformed cell lines, completely blocks oncogenic p21-induced oocyte maturation but has much less effect on insulin-induced maturation (40). Only at high doses of this compound is a maximal level of about 70 percent inhibition of insulin-induced oocyte maturation achieved. This maximal level of inhibition is maintained independently of the dose of insulin.

Furthermore, a compound that is known to inhibit

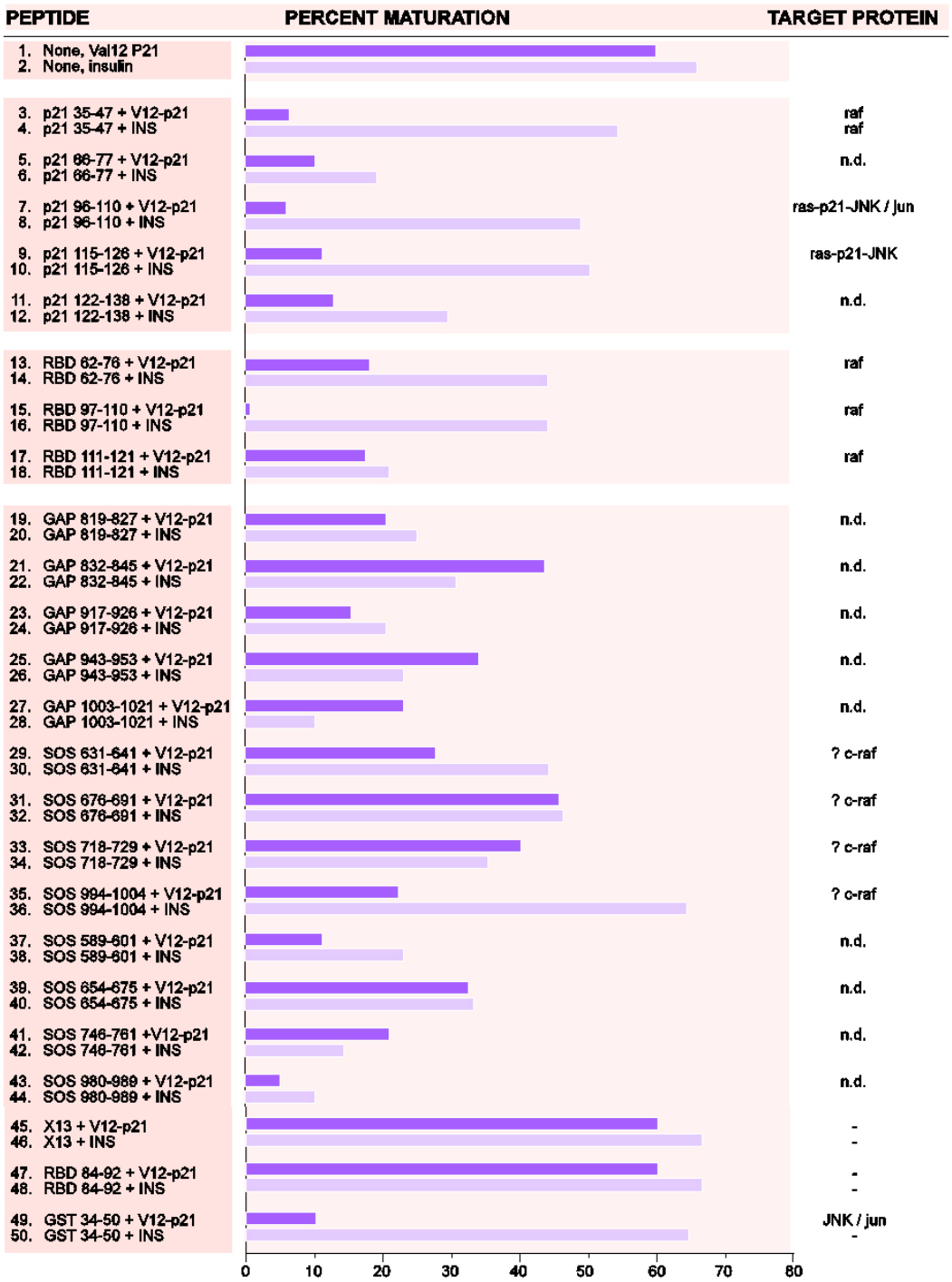

Figure 4. Effects of effector domain peptides, identified from conformational energy calculations on wild-type and oncogenic *ras*-p21 proteins alone and in complexes with known target and/or regulatory proteins, on oncogenic *ras*-p21- and insulin-induced oocyte maturation. Conditions are given in the left-most column of this figure. The percent oocyte maturation is given as a horizontal bar graph in the middle column; and target proteins for different peptide inhibitors are given in the right-most column of this figure. In this column, the target protein is listed if it has been identified; if it has not been definitively identified, but there is supporting evidence that it is a target protein, the protein is listed with a question mark; if the target protein(s) has (have) not been identified, n.d. signifies that they have not as yet been determined. The data are arranged as sets of two for each peptide assayed. The effects of each peptide on oncogenic *ras*-p21 (V12-p21)- and insulin (INS)-induced maturation are given in that order. The two top-most conditions are controls for Val 12-*ras*-p21- and insulin-induced oocyte maturation in the absence of peptide. Results with negative control peptides are shown for X13 (from cytochrome P450) and *raf* 84-92 peptides are shown in condition sets 45-46 and 47-48, respectively. Since, for these latter two peptides, no target protein is involved, a dash is listed in the right-most (target protein) column.

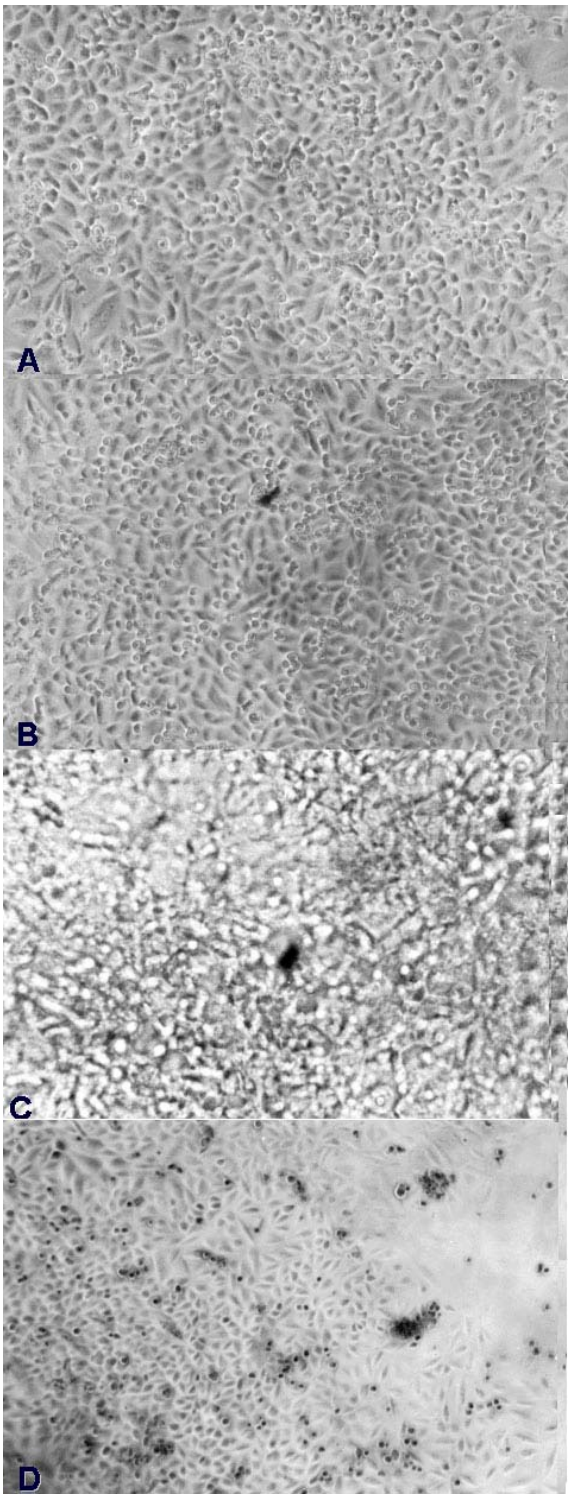

Figure 5. Effects of *ras*-p21 96-110-Leader peptide on TUC-3 pancreatic cancer cells and on untransformed BMRPA1 cells Panel A, untreated BMRPA1 cells; panel B, BMRPA1 cells. treated with *ras*-p21 96-110-Leader peptide for two weeks. Panel C, untreated TUC-3 pancreatic cancer cells showing typical "heaping up" of cells; Panel D, TUC-3 pancreatic cancer cells treated with *ras*-p21 96-110-Leader peptide for two weeks, showing reversion to BMRPA1-like cells (panels A and B).

the activity of protein kinase C (PKC) with high selectivity, a staurosporine derivative called CGP-41-251, but not an inactive control staurosporine derivative, CGP 42 700, strongly blocks oncogenic *ras*-p21 induction of oocyte maturation (41). That CGP 41 251 blocks oncogenic p21 by blocking PKC activation is suggested by our finding that the dose-response curves for inhibition by this agent of oncogenic-*ras*-p21- and PKC-induced oocyte maturation are superimposable. Also, the IC_{50} for this inhibition intracellularly is similar to that for the *in vitro* inhibition of PKC activation by this agent (42). Since PKC induces oocyte maturation that is not inhibited by the inactivating anti-p21 antibody, Y13-259, while *ras*-p21-induced maturation is blocked by CGP-41-251, PKC must lie downstream of oncogenic p21 on the oncogenic *ras* signal transduction pathway (42).

In contrast, CGP 41 251 has virtually no effect on insulin-induced maturation except at high concentrations where a maximum of 40 percent inhibition is reached (41, 42). As with AzTyr, this maximal level of inhibition is maintained independently of the concentration of insulin and the extent of maturation that it induces.

Based on these prior results, we hypothesized that oncogenic *ras*-p21 utilizes a signal transduction pathway that requires specific targets like PKC. Activated wild-type *ras*-p21 also utilizes these targets but also activates alternate pathways that do not require them. As signal transduction proceeds downstream, the wild-type pathways branch increasingly so that progressively less inhibition by agents that interfere with signaling by oncogenic *ras*-p21 is achieved (42).

Thus normal p21 would send proliferation signals by a number of different pathways, i.e., signal transduction by normal p21 is "plastic." In contrast, oncogenic p21 would transmit its signals by a more stereotypical pathway that has many fewer "escapes." It should be possible, therefore, to block oncogenic proliferative signaling selectively without affecting normal proliferation signals.

4.1.4. Critical Targets of Oncogenic *ras*-p21

Critical Targets of Oncogenic *ras*-p21 Are JNK and *jun* Proteins. In experiments designed to detect target proteins with which oncogenic p21 interacts preferentially, we prepared a photoaffinity-labeled Val 12-p21 protein that we introduced into NIH 3T3 cells quantitatively. This labeled protein has a photo-activatable group resulting in a highly reactive nitrene species that inserts covalently into any protein to which p21 is bound. We identified a protein of with a molecular mass of 43 kDa which possessed kinase activity (43). This protein powerfully induced oocyte maturation by itself (44).

Immunoprecipitation of *ras*-p21 from a fibroblast (3T3/4A) cell line blotted positively for *jun*-N-terminal kinase, JNK-1, Mr 46 kD and for its substrate, *jun* protein (45). We have confirmed this result in in *vitro* experiments in which we have prepared beads of either cloned and overexpressed JNK or *jun* and incubated them with cloned

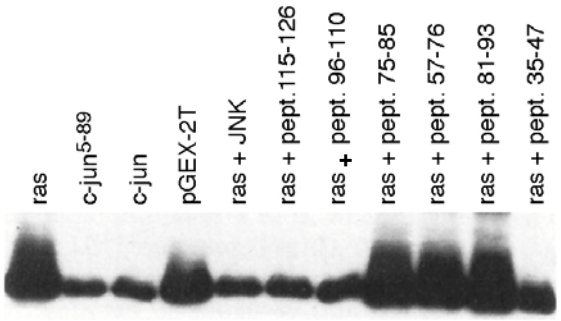

Figure 6. Effects of effector peptides, identified from conformational energy calculations, on the binding of Val 12-*ras*-p21 protein to bead-bound JNK. In these experiments, Val 12-*ras*-p21 was incubated with bead-bound p-GEX-JNK alone (first lane); in the presence of the positive control proteins JNK and *jun*, and the negative control pGEX fusion protein (that does not bind to *ras*-p21 or to JNK); and in the presence of *ras*-p21 effector peptides. After incubation, the JNK-containing beads were washed and subjected to SDS PAGE and blotted for *ras*-p21. Val 12-*ras*-p21 by itself (first lane) binds strongly to the JNK beads (strong Val 12-*ras*-p21 signal). This effect is blocked by addition of JNK (but not by pGEX-2T construct negative control protein), the amino terminal 5-89 regulatory domain of c-*jun* and c-*jun.* This effect is reproduced by the 115-126 and 96-110 peptides but not by the other *ras*-p21 peptides. Adapted from ref. 46.

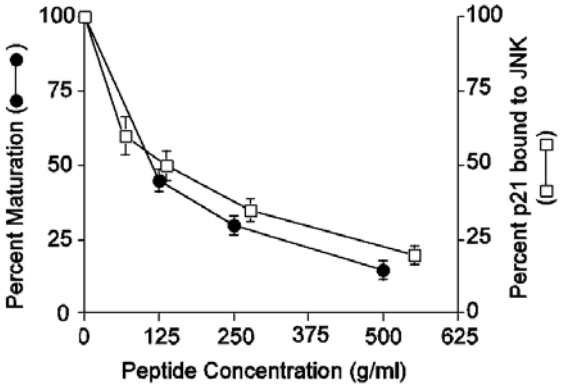

Figure 7. Dose-response curves for inhibition by PNC-2, the *ras*-p21 96-110 peptide, of Val 12-*ras*-p21-induced oocyte maturation (left ordinate) and the binding of Val 12-*ras*-p21 to bead-bound JNK (right ordinate).

and overexpressed oncogenic or normal p21 (45, 46). Oncogenic p21 binds with over a four-fold increase in affinity and greatly accelerates the phosphorylation of *jun* by JNK; activated normal p21 stimulates this phosphorylation to a much lower extent (45).

Using the *in vitro* system, we have incubated both bead-bound JNK and *jun* proteins with Val 12-p21 in the presence of each of the *ras*-p21 peptides to determine if one or more of them inhibits the interaction (45, 46). As shown in Figure 6 for bead-bound JNK incubated with Val 12-p21, two peptides, the 96-110 and the 115-126 peptides, strongly blocked this interaction to the same extent as added JNK or *jun* positive control proteins. The 96-110 peptide also blocked the binding of Val 12-p21 to bead-bound *jun* (45, 46).

Importantly, as shown in Figure 7, the dose-response curve for inhibition, by the *ras*-p21 96-110 peptide, of Val 12-p21-induced oocyte maturation, superimposes on that for its inhibition of the binding of Val 12-p21 to bead-bound JNK (7). This result suggests that an important site of action of the *ras*-p21 96-110 peptide is the Val 12-p21-JNK interaction.

Studies Further Confirm that Oncogenic ras-p21 Interacts with JNK/jun Preferentially. That JNK/*jun* is a vital target of oncogenic *ras*-p21, as opposed to the activated wild-type protein, has been further confirmed in a number of experiments (7). First, oocytes induced to mature to the same extent over a 24 hr period either by injected Val 12-p21 or by insulin, were lysed, subjected to SDS PAGE and then blotted for activated (phosphorylated) JNK. As can be seen in the left panel of Figure 8, only in the Val 12-p21-treated oocytes was there a large band (lane 3); in insulin-treated oocytes the level of activated JNK was much lower (lane 4). Furthermore, oocyte maturation correlates with JNK activation in Val 12-p21-injected oocytes but not in insulin-treated oocytes (47).

As shown in the right panel of Figure 8, Western blots, using the same antibody, of lysates from oocytes co-injected with oncogenic *ras*-p21 and the p21 96-110 effector peptide, that blocks oncogenic *ras*-p21-JNK interactions and also blocks oocyte maturation, show markedly diminished activated JNK (lane 3, right) (47). This result supports the importance of JNK activation on the oncogenic *ras*-p21 pathway.

Second, we have identified a new highly selective protein inhibitor of activation of *jun* by JNK. This protein is glutathione-S-transferase-pi (GST-pi), which we have found binds only to *complexes* of JNK-*jun* and blocks *jun* activation (25, 48). Co-injection of this protein together with Val 12-p21 results in total blockade of oocyte maturation, but injection of this protein into oocytes which were then subsequently incubated with insulin has no effect on insulin-induced maturation (49). This result further confirms that oncogenic *ras*-p21, in contradistinction to its wild-type counterpart protein, requires JNK/*jun* as critical targets on its pathway. As we describe below, we have used conformational analysis to identify domains of GST-pi that are involved in this signal transduction function.

Third, co-injection of JNK with Val 12-p21 results in a synergistic enhancement of oocyte maturation while injection of JNK or *jun* into insulin-treated oocytes results in a *diminution* of maturation (50). If activated cellular wild-type *ras*-p21 interacted with JNK in the same manner as the oncogenic protein, enhanced maturation should have been observed.

These experiments support the conclusions that both JNK and *jun* are critical direct targets of oncogenic but not activated wild-type *ras*-p21 and that the *ras*-p21 96-110 and 115-126 peptides block the interaction between oncogenic *ras*-p21 and JNK/*jun*. The *ras*-p21 35-47 peptide,

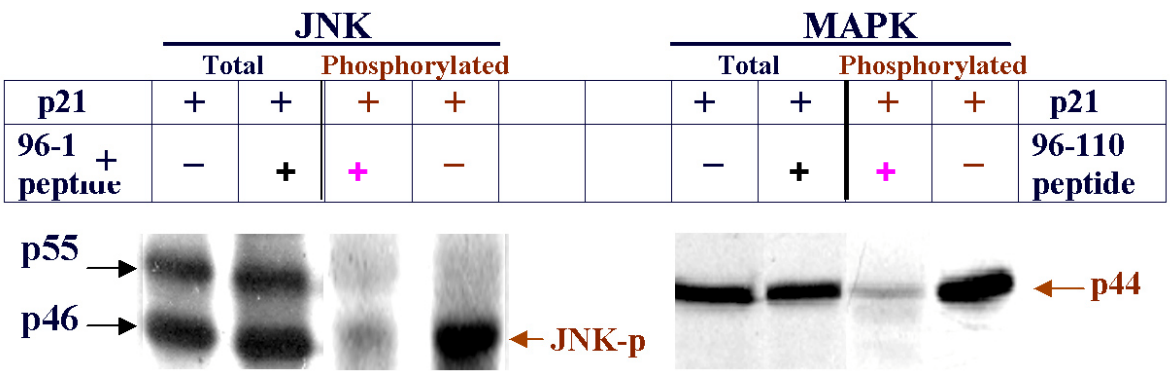

Figure 8. Left blots. Total JNK (lanes 1 and 2) and activated-phosphorylated JNK (lanes 3 and 4) in oocytes that were induced to mature by oncogenic *ras*-p21 (lanes 1 and 3) and by insulin (lanes 2 and 4). p P46 and p55 are for JNK-1 and 2, respectively. Phosphorylated JNK migrates between these two bands. Right blots. Effects of co-injection into oocytes of *ras*-p21 96-110 peptide with oncogenic *ras*-p21 on total JNK (lane 2) and activated-phosphorylated JNK (lane 3). Lanes 1 and 4 are controls, corresponding to the conditions in lanes 1 and 3 in the left blots, and show the effects on injection of oncogenic *ras*-p21 into oocytes in the absence of peptide on total JNK and activated-phosphorylated JNK, respectively.

which also inhibits oncogenic *ras*-p21 with high selectivity, does not block these interactions. This result correlates with our finding that the 35-47 peptide does not inhibit JNK-induced oocyte maturation. As we discuss in the next section, this peptide interacts with the amino terminal regulatory domain of *raf*.

4.1.5. The *raf*-MEK-MAP Kinase Pathway Is Also Critical for Oncogenic *ras*-p21

Microinjection into oocytes of high levels (100 micro g/ml) of a plasmid that constitutively expresses c-*raf* protein induces high levels of oocyte maturation (34). This is completely inhibited by another plasmid that encodes a dominant negative *raf* (dn-*raf*) protein containing an inactive kinase domain (34). This construct also strongly blocks oocyte maturation induced both by oncogenic *ras*-p21 and by insulin, suggesting that *raf* is a common target of both oncogenic and activated wild-type *ras*-p21 (34).

On the other hand, a construct encoding MAP kinase (ERK-1 and 2)-specific phosphatase, MKP-1T4, strongly inhibits oncogenic *ras*-p21-induced oocyte maturation but inhibits insulin-induced maturation much more weakly. This result suggests that activated MAP kinase may be more important for oncogenic *ras*-p21 than for the activated wild-type protein (34).

We have confirmed this conclusion by blotting, with antibody to activated MAP kinase, whole cell lysates from oocytes induced to mature, over a 24 hr period, either by microinjection of oncogenic *ras*-p21 into oocytes or incubation of oocytes with insulin. Only lysates from oocytes induced to mature with oncogenic *ras*-p21 showed a prominent band (47). Thus it appears that *raf* is a necessary target for both oncogenic and wild-type *ras*-p21 but is a branch point, i.e., oncogenic *ras*-p21 stimulates it to activate the MEK-MAP kinase pathway while activated wild-type *ras*-p21 activates it to interact with alternate pathways.

This conclusion is further supported by recent experiments seeking to identify the site of action of the *ras*-p21 35-47 peptide. This peptide strongly blocks oocyte maturation induced by c-*raf* (51). However, it does not block oocyte maturation that is induced by a plasmid encoding *raf*-BXB, which is an oncogenic, constitutively activated form of *raf* that lacks the amino terminal regulatory domain (52). These results suggest that the *ras*-p21 35-47 peptide acts by binding to the amino terminal regulatory domain of *raf* and blocks its activation and/or its activation of downstream targets like MEK.

This result is paradoxical in that blockade of *raf* by dn-*raf* blocks oocyte maturation induced both by oncogenic and insulin-activated wild-type *ras*-p21; yet blockade of c-*raf* by the p21 35-47 peptide appears not to affect insulin-induced maturation. Yet insulin-induced maturation depends on *raf*.

This apparent paradox can be resolved if the 35-47 peptide interacts with *raf* in such a way as to block its activation of downstream targets like MEK that are critical to oncogenic *ras*-p21 but not to the activated wild-type protein, but not so as to block its interaction with alternate pathway targets for the activated wild-type protein. Our computed results for complexes of wild-type and oncogenic *ras*-p21 proteins with the RBD of *raf* provide further insights into this question as we now discuss.

4.2. Conformational analysis of wild-type and oncogenic *ras*-p21 bound to target proteins

The x-ray crystal structures of several proteins that interact with *ras*-p21 have become available. Among these are the *ras*-binding domain of *raf* (10), GAP (11) and SOS (12) proteins. While *raf* is a downstream target of activated *ras*-p21, the role of GAP and SOS as signaling, in addition to their being regulatory, proteins is less clear. Injection of purified GAP into oocytes induces phospholipid synthesis and activation of phospholipase (H. F. King, personal communication); as shown in Figure 1, SOS interacts with MEK such that high levels of MEK block SOS activity. In addition, SOS interacts with grb-2, which is necessary for SOS activation (Figure 1). Thus

there is some evidence that both of these proteins are involved in signal transduction.

4.2.1. Calculations Reveal New Peptide Domains in *ras*-p21 Targets Involved in Cell Signaling

To explore this question further, we have performed similar calculations to those described in Section 1a above on these *ras*-p21 complexes. In these calculations, we have computed the average structures of wild-type and oncogenic *ras*-p21 bound to each of the above three proteins and have superimposed their average structures to identify domains of the target proteins-and other domains of *ras*-p21 in these complexes-that undergo structural changes when bound to oncogenic *ras*-p21. As with *ras*-p21, we then synthesized peptides corresponding to these domains and tested them for their abilities to block oncogenic and insulin-activated wild-type *ras*-p21-induced oocyte maturation.

The purpose of this protocol is to detect domains of the *ras*-p21 targets that may be involved uniquely in oncogenic *ras*-p21 signaling and that therefore selectively inhibit oncogenic *ras*-p21. As described in the ensuing sections, we have identified a number of such peptides.

4.2.2. Interpretation of Results

As described in the following sections below, we have found that certain domain peptides inhibit both oncogenic *ras*-p21- and insulin-induced oocyte maturation despite changes in the structures of these domains. This observation may be due to one or more of the following phenomena.

First, as we discuss in the ensuing sections, most domain peptides that inhibit both maturation-promoting agents change mainly their *positions* on the surface of their respective target proteins; their conformations are quite similar, i.e., their structures are superimposable. Thus each may still be exposed on the surface of the protein and may be able to interact with their protein targets.

Second, the domains themselves may not interact with target proteins but rather may interact with other domains of the protein that are critical in interacting with other target proteins intracellularly. In complexes with both oncogenic and activated wild-type proteins, these domains may move away from these critical segments, exposing them, thereby allowing them to interact with critical target proteins. Injection of the domain peptide into oocytes may result in the binding of the segment to the common critical domains, once again blocking them so that they cannot interact with these target proteins.

Third, although we have identified the sites of interactions of a number of these peptides intracellularly, the sites of interaction of some of these peptides have not as yet been defined; it is possible that they can interact with target proteins other than those contacted by their parent proteins. These other proteins may be critical to signaling by both oncogenic and wild-type *ras*-p21 proteins.

It should also be noted that it is possible that a peptide does not affect the ability of either agent to induce oocyte maturation. This result would indicate either that the peptide does not adopt sufficient native-like three-dimensional structure, rendering it ineffective or that the peptide domain has no importance in signaling, despite its change in conformation in the two complexes. As we show in the next sections, all peptides tested thus far have blocked mitogenic signaling by either agent or both agents, but do not affect progesterone-induced maturation, that does not occur via a *ras*-dependent pathway, indicating that they exert effects on signal transduction by *ras*-p21 and that their parent proteins are involved in mitogenic signaling.

4.2.3. *ras*-p21-*raf* RBD Complexes

The *raf*-p74 protein, containing over 800 amino acid residues, has an amino terminal regulatory domain consisting of residues 51-131 that bind to activated *ras*-p21, hence the term *ras*-binding domain (RBD) (10). Deletion of all or large segments of this domain results in constitutive activation of *raf*, resulting in its becoming oncogenic. *ras*-p21 also binds to *raf* in a cysteine-rich region containing residues 139-184 of *raf* (53) and the region of *raf* around residue 257 (54). The crystal structure of residues 55-131 of the RBD has been determined bound to a *ras*-p21 inhibitory G-protein called rap-1A (10). This protein has over 50 percent sequence identity and over 90 percent sequence homology to *ras*-p21 (10).

Interestingly, the RBD segment has been found, using two-dimensional NMR, to fold by itself to a structure that is directly superimposable on the protein ubiquitin (10 and references therein), the vital catabolic regulatory protein to which it has only low sequence homology. Its structure bound to rap-1A is identical indicating that, at least in the crystal, the binding of rap-1A does not alter its structure.

Furthermore, the structure of rap-1A in this complex is identical to that of free *ras*-p21 bound to GTP suggesting that the structure of rap-1A is close to that of wild-type *ras*-p21 and that there is little change in structure when either rap-1A or, putatively, *ras*-p21, binds to the RBD (10). In the complex, rap-1A interacts directly with the RBD using its switch 1 (residues 32-47) domain, mainly a beta-sheet, that makes multiple polar contacts with the beta-2 domain, residues 63-71, of the RBD and, additionally, with RBD residues Lys 84 and Arg 89 (10).

We have generated the structure of wild-type *ras*-p21 such that it overlay that for rap-1A in its complex with the RBD. Both of these structures were then subjected to energy minimization and the resulting energy-minimized structures were the starting structures for molecular dynamics calculations (55).

When the average structures for these complexes were computed from the molecular dynamics calculations and were then superimposed, we found that the overall complexes exhibited the same folding pattern but differed in structure in discrete regions. In particular, three regions of the RBD were found to undergo major structural changes: residues 62-76 of the interface between rap-1A or wild-type *ras*-p21 and the RBD, 97-110 and 111-121 (55).

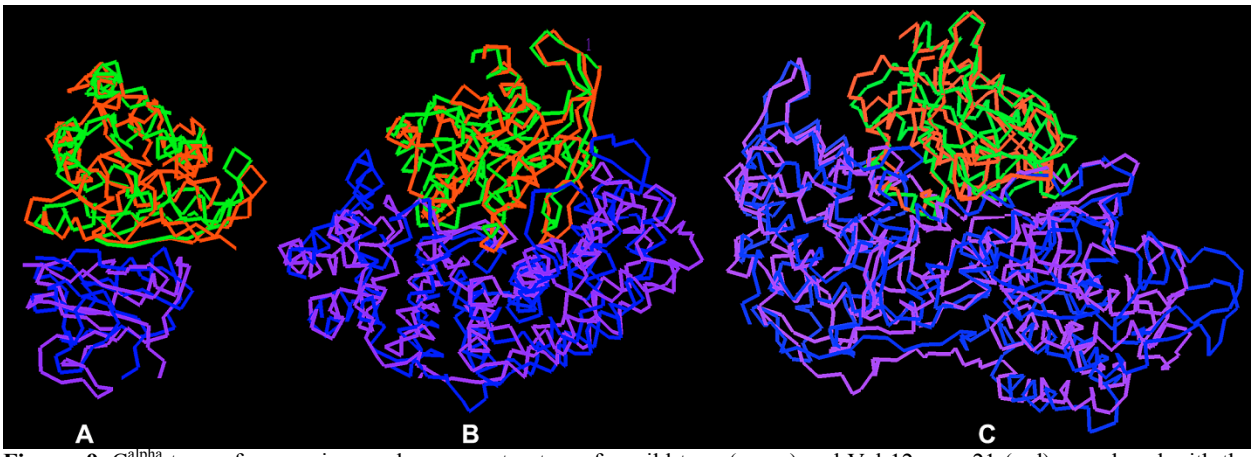

Figure 9. C^{alpha} traces for superimposed average structures for wild-type (green) and Val 12-*ras*-p21 (red) complexed with the RBD of *raf* (A), GAP (B) and SOS (C). In each complex, the target protein bound to oncogenic *ras*-p21 is colored dark blue while the target protein bound to the wild-type protein is purple.

Since binding of rap-1A to *raf* competitively blocks the binding of *ras*-p21 to *raf* and blocks *ras*-p21-induced signal transduction, these domains appear to be important in the activation of *raf* by *ras*-p21. These segments would appear to be important in activation of *raf* since they are the only domains that change structure significantly.

We further analyzed the structures of these three peptide domains that change conformation in the RBD complexes and found that the largest differences in structures are caused by their displacements on the surface of the protein. When superimposed individually, their conformations were very similar (55, 56). Thus differences in their activities in cells may be due to differences in the *dispositions*, rather than the conformations, of these peptide domains.

4.2.3.1. RBD Peptides Block *ras* Signaling

We then synthesized peptides corresponding to these three *raf* sequences and co-injected each of them with oncogenic *ras*-p21 protein into oocytes and also injected each of them into oocytes subsequently incubated with insulin (57). As shown in Figure 4, all three peptides blocked oocyte maturation induced by oncogenic *ras*-p21 (entries 13, 15 and 17). The 62-76 peptide (entry 14) inhibits both agents but blocks oncogenic *ras*-p21 to a greater extent (entry 13) while the 111-121 peptide inhibits oncogenic *ras*-p21- and insulin-induced maturation to almost the same extent (entries 17 and 18, respectively).

On the other hand, as shown in Figure 4, neither microinjection of the X13 negative control peptide (entries 45 and 46) nor of a control peptide from the RBD corresponding to residues 84-92, which does not change conformation when the two complexes are superimposed (entries 47 and 48), resulted in inhibition of oocyte maturation induced by either agent. This suggests that the inhibition by these peptides is specific. That the inhibitory effects are *ras*-specific is supported by our finding that none of these peptides blocked progesterone-induced oocyte maturation, a *ras*-p21-independent process (6) (not shown).

All three of these peptides also inhibit c-*raf*-induced oocyte maturation but have no effect on JNK-induced maturation (33, 51), consistent with our conclusion that they block c-*raf* specifically. Since the RBD 62-76 peptide contains almost all of the residues that interact with rap-1A and *ras*-p21 at the interface between the two proteins, it is not surprising that the 62-76 segment blocks signal transduction both by oncogenic and activated wild-type *ras*-p21. Since the RBD 111-121 peptide also blocks c-*raf*-induced maturation, its inhibition may be due to its uncovering common domains either in the RBD or in the whole *raf* protein, which is required for activation of *raf* itself or of downstream targets. It is also possible that this domain itself may be required for activation of a common target, as yet unidentified.

4.2.3.2. The RBD 97-110 Domain Peptide Blocks Oncogenic *ras*-p21 Selectively

On the other hand, as shown for entries 15 and 16 in Figure 4, the RBD 97-110 peptide blocks oncogenic *ras*-p21-induced maturation to a much greater extent than it blocks insulin-induced maturation (57). Thus this peptide appears to be selective for inhibiting the oncogenic form of *ras*-p21.

To analyze this result further, we performed molecular dynamics calculations on the Val 12-p21 protein bound to the RBD. We then superimposed the average structure for this complex on that for the wild-type *ras*-p21-RBD complex (56). The results are shown in Figure 9A, where it can be seen that both proteins in each complex have the same overall three-dimensional fold but differ regionally. One dramatic change in domain disposition occurs at the surface 97-110 loop. As shown in Figure 10A, this loop (colored red) flips 180 degrees over the surface of the protein in the oncogenic complex, resulting in a 15 A displacement from the loop in the wild-type complex (colored green). This displacement appears to be critical for the activation of *raf* by oncogenic, but not activated wild-type, *ras*-p21.

Comparison of the average structures of the *ras*-p21 protein in both average structures for oncogenic and wild-type *ras*-p21 bound to the RBD shows a low rms deviation (1.4 A) compared with the relatively high

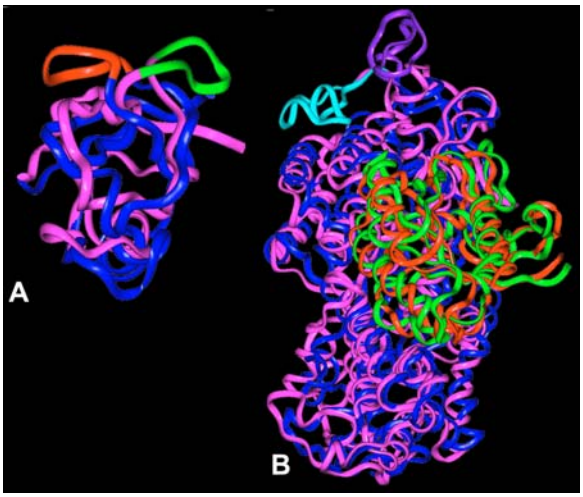

Figure 10. Superimposed ribbon structures showing displacement of surface loops involved in signal transduction in *raf* (A) and SOS (B) proteins. In A, only the *raf* RBD structure from the oncogenic complex (blue) is superimposed on that from the wild-type complex (pink). The critical 97-110 loop in the oncogenic complex is red while that in the wild-type complex is green. In B, the entire superimposed structures for *ras*-p21-SOS complexes are shown using the same color scheme as in Figure 9. The displacement of the 654-675 loop (cyan in the wild-type complex, dark purple in the oncogenic complex) is shown.

rms deviation (4.7 A) for the RBD component. In this comparison, we found that the 32-47 segments of *ras*-p21 differ significantly in their carboxyl terminal domains, i.e., residues 44-47 (56), indicating that these residues are important in determining the function of the complex. Since this domain is the major *ras*-p21 domain that makes contact with the RBD, these differences would appear to cause the major changes in structures undergone by the RBD itself. Thus the 97-110 domain of the RBD appears to be vital in a molecular switching function in which the positioning of this domain determines the pathways that are activated by *raf*.

4.2.3.3. How the *ras*-p21 35-47 Peptide Might Block Oncogenic *ras*-p21 Selectively

As noted in Section 1e above, the *ras*-p21 35-47 peptide selectively blocks oncogenic *ras*-p21 by blocking c-*raf* activation. If this peptide were to bind to the RBD of *raf* in a mode like that for activated wild-type *ras*-p21, especially for residues 44-47, and if wild-type *ras*-p21 can bind to accessory *ras* binding sites in *raf* such as 139-184 of *raf* (53, 54) and the region of *raf* around residue 257 (33) (Section 2c above), this complex would result in a normal activation of *raf* causing displacement of the RBD 97-110 domain to occur as it does in binding to the wild-type protein. This scenario predicts that a ternary complex would form in which *raf* would simultaneously bind to *ras*-p21 35-47 peptide and wild-type *ras*-p21 protein.

4.2.3.4. Conclusions

Overall, conformational analysis of the *ras*-p21-*raf* RBD complex has revealed effector domains, peptides from which inhibit *ras* signaling in a specific manner. One of these peptides, corresponding to the 97-110 RBD segment, further selectively inhibits oncogenic *ras*-p21. Since this peptide blocks c-*raf*-induced signaling, *raf* may be a critical branch point in *ras* signaling in which oncogenic and activated wild-type *ras*-p21 cause *raf* to activate different pathways despite the fact that it is a common target of both proteins. Since the RBD 97-110 peptide selectively blocks oncogenic *ras*-p21, it may be useful in blocking oncogenic *ras*-p21 protein-induced tumor proliferation but not normal cell growth.

4.2.4. *ras*-p21-SOS Complex

As noted in Section 1 above, binding of SOS to wild-type *ras*-p21 induces exchange of GDP for GTP, resulting in activation of *ras*-p21. SOS is a large protein that contains 1044 amino acid residues (12). The domain containing residues 568-1044, which is almost all alpha-helical, is involved in interacting with *ras*-p21. This domain is itself divided into two further sub-domains: a structural sub-domain, residues 568-751, consisting of six alpha-helices 1-6, apparently required to maintain the overall structure of the whole *ras*-binding domain; and the 752-1044 sub-domain, containing helices A-K, and including the residues that make contacts with *ras*-p21, most notably the H-helix (residues 925-946) (12).

Unlike the other proteins with which *ras*-p21 interacts, SOS makes multiple contacts with a wide variety of different domains of *ras*-p21 (12). These include the switch 1 domain (residues 32-47) and another adjacent domain involving residues 25-31, the switch 2 domain (residues 55-75), residues 95-105 that overlaps with the *ras*-p21 96-110 peptide domain (see Sections 1a, b and d above) and residues 118-123 containing the *ras*-p21 residues that are involved in binding to the guanine ring of GDP and GTP and are contained in the *ras*-p21 115-126 effector domain (see Sections 1a, b and d above) (11, 12).

From the x-ray structure of residues 1-166 of *ras*-p21 bound to residues 568-1044 of SOS (12), there are large changes in the conformations and dispositions of both *ras*-p21 switch 1 and 2 domains. For example, comparison of the conformation of the switch 1 domain in *ras*-p21 bound to SOS with that in free *ras*-p21 or *ras*-p21 bound to GAP shows an overall rms deviation of over 5Å. In addition, Phe 28 is found move 9.6 Å away from its position in the unbound *ras*-p21 protein.

To explain how SOS promotes nucleotide exchange, it has been noted in the x-ray crystal structure that certain favorable contacts occur between *ras*-p21 and SOS that replace those between *ras*-p21 and GDP/GTP (12). For example, Leu 938 from the H alpha-helix of SOS lies near Ala 59, from the switch 2 region of *ras*-p21, resulting in a hydrophobic pocket; and Glu 942, also from the H alpha-helix of SOS, has polar interactions with Ser 17 from the p21 switch 2 domain (12). Both of these contacts are thought to replace the favorable interactions of these residues with the phosphate moieties of GDP/GTP and the magnesium ion (12), resulting in loss of nucleotide binding. However, the guanine ring of GTP can still bind to

ras-p21 allowing it ultimately to displace SOS from the *ras*-p21-SOS complex (12).

Since SOS interacts with many *ras*-p21 domains including those like residues 96-110 and 115-126, that we have formerly identified as being important effector domains for oncogenic *ras*-p21 (7, 45, 46), we have investigated whether SOS may contain regions that may be critical to oncogenic *ras*-p21 signaling uniquely. We have therefore performed molecular dynamics calculations on complexes of SOS with wild-type and oncogenic *ras*-p21 to identify such domains.

4.2.4.1. Results of Molecular Dynamics Calculations on *ras*-p21-SOS Complexes

We have performed these calculations in the same manner as for *ras*-p21-RBD complexes described in the preceding section. It should be noted that in the x-ray structure of *ras*-p21-SOS, three loop domains of SOS were structurally undefined, viz, residues 591-596, 654-675 and 742-751 (12), all in the structural domain. We have performed computations in the absence of these three segments (58) and then in the presence of these segments, which we subsequently modeled into the overall structure (59).

Superposition of the average structures for oncogenic *ras*-21-SOS on that for wild-type *ras*-p21-SOS including the three loop domains is shown in Figure 9C. As with the *ras*-p21-RBD complex, shown in the same figure, 9A, both structures can be seen to contain the same overall chain fold but differ structurally in specific domains. Major changes in conformation and/or disposition occur at residues 631-641, 676-691, 718-729 and 994-1004 in SOS complexes without the loops included and at these residues and in segments containing or contiguous with the three loop segments at residues 591-596, 654-675 and 742-751 and, additionally at residues 980-989. All of these domains occur in the structural sub-domain of SOS except for the 980-989 and 994-1004 peptides that occur in the *ras*-interacting domain.

4.2.4.2. SOS Domain Peptides Block *ras*-p21-Induced Signal Transduction.

We have synthesized peptides corresponding to all of these eight SOS domains and have microinjected them into oocytes either together with oncogenic *ras*-p21 or into oocytes that were subsequently incubated with insulin (60, 61). As shown in entries 29-44 of Figure 4, all of these peptides inhibit oncogenic *ras*-p21, and many of them also inhibit insulin. All of the peptides from the structural sub-domain of SOS, including the three loop peptides, inhibit both agents. On the other hand, the two peptides from the *ras*-interacting sub-domain, 980-989 (entries 43 and 44) and especially the 994-1004 peptide (entries 35 and 36), inhibit oncogenic *ras*-p21 to a greater extent. Also, the two latter peptides are the most potent inhibitory peptides from all of the SOS domains (60, 61).

A surprising result from these calculations concerns the loop segment 654-675. This domain was modeled into the original energy-minimized x-ray structure by its homology (70 percent) to a segment from *V. cholera* neuraminidase whose x-ray structure has been determined (62). In this protein, this segment is buried in the interior of the protein as part of a series of beta sheets with which it forms multiple contacts. In the starting conformation of this segment and in the two average structures of *ras*-p21-SOS, this segment occurs on the surface of the protein where it may bind to complementary segments of other target proteins.

As shown in Figure 10B, in the superimposed average structures, much like the 97-110 domain of the RBD of *raf*, the 654-675 SOS domain undergoes a large (20 A) displacement from one face of the protein to the opposite face on the surface and yet retains a similar conformation (59). It may be seen from entries 39 and 40 in Figure 4 that, unlike the RBD 97-110 peptide (entries 15 and 16), this peptide inhibits both oncogenic *ras*-p21- and insulin-induced maturation to about the same extent (60).

These results suggest that all eight domains of SOS may be involved in cell signaling. The two *ras*-interacting domain peptides may be involved with oncogenic *ras*-p21-specific signaling pathways while the peptides from the structural domains affect common signaling pathways despite the large displacements. All of the latter segments retain their conformations; i.e., they are superimposable on one another as the isolated domains from the two complexes.

As discussed in Section 4.2.2 above, these domains may interact with common target proteins on the surface of SOS, independently of their positions on the surface; or in changing position, they may expose other domains of SOS that actually interact with a common target. Since these segments occur in the structure-stabilizing sub-domain, their changes in position may activate the *ras*-interacting sub-domain of SOS. Alternatively, these peptides may block signal transduction proteins other than SOS on the *ras* pathway.

4.2.4.3. Specificity of Inhibition.

Inhibition of oocyte maturation by all of these peptides appears to be specific for *ras*-induced pathways since none of these peptides was found to inhibit progesterone-induced oocyte maturation, that is *ras*-independent (6) as noted in the Introduction. In addition, we have synthesized an SOS domain corresponding to residues 809-815 that does not change conformation when the two *ras*-p21-SOS structures were superimposed (58, 59) (M.R. Pincus, unpublished data). This peptide affects neither oncogenic *ras*-p21- or insulin-induced oocyte maturation.

Identification of the sites of inhibition of each SOS peptide is more complicated. Unlike with c-*raf*, SOS does not by itself result in high levels of oocyte maturation (H.-F. Kung, personal communication). Thus proof of functional inhibition of SOS by these eight SOS proteins requires other functional studies. One such study might consist of injecting into oocytes recombinant forms of SOS that lack each of these eight domains to determine if they promote nucleotide exchange but still act as dominant negative inhibitors of Val 12-*ras*-p21- and insulin-induced maturation.

We are currently preparing such mutant SOS proteins including mutant forms that have residues 980-989 and 994-1004 deleted. If SOS is vital to oncogenic *ras*-p21 signaling and these mutants are functional, they should block oncogenic *ras*-p21- but not insulin-induced oocyte maturation.

4.2.4.4. Conclusions

Overall, conformational analysis of *ras*-p21-SOS complexes has revealed eight potential effector domain peptides, two of which (980-989 and 994-1004) selectively block oncogenic *ras*-p21-induced oocyte maturation. If these two peptides block the interaction of SOS with target proteins, then SOS is implicated as a target in *ras*-induced mitogenic signal transduction. Since the two peptides selectively block oncogenic *ras*-p21, SOS, like *raf*, may be a branch point in signal transduction by oncogenic and activated wild-type *ras*-p21.

4.2.5. *ras*-p21-GAP Structures

Binding of *ras*-p21 to all of its targets except GAP results in an activation process in which no covalent catalysis occurs. However, GAP induces about a one thousand-fold increase in the catalytic rate for *ras*-p21-bound GTP hydrolysis (11). Thus a major objective in obtaining the x-ray structure of p21-GAP was to determine the possible catalytic mechanism for hydrolysis of p21-bound GTP by GAP. To help answer this question, therefore, a p21-GAP complex was crystallized in which p21 was bound to GDP and AlF_3, that is thought to "mimic" the gamma-phosphate of GTP in a trigonal bi-pyramid transition state-like structure, thought to be the rate-determining transition state in GTP hydrolysis (11). It should be noted, however, that AlF_3 is a planar structure which does not contain apical anionic atoms as would be expected to exist in a trigonal bipyramidal phosphate transition state structure.

In the structure of the *ras*-p21-GAP complex (11), GAP 334 (containing residues 718-1037), like SOS, is an all-alpha-helical protein in which there are eight helical domains (designated as alpha1$_c$-alpha8$_c$ separated by six loops, designated as L1$_c$-L6$_c$). Of these, the domains that contact p21 are alpha6$_c$, alpha7$_c$, L1$_c$ and L6$_c$. L1$_c$ is called the "finger loop" because it contain residues that extend into the GTP binding site of p21, particularly Arg 789, which interacts with Gly 12, Gln 61 and the fluoride atoms of AlF_3 (11).

This residue has therefore been postulated to stabilize incipient negative charge on the oxyanion of the gamma-phosphate in the rate-determining transition state (11). It also interacts with Glu 31 of the switch 1 domain via a water molecule. Since Arg 789 and Gln 61 lie close to one another and to the F atoms of AlF_3, the NH_2 moiety of Gln 61 has been postulated to be involved in hydrogen-bonding to the oxyanionic transition state through hydrogen-bonding. This would explain why substitution of most amino acids for Gln 61, other than Glu, which has a similar side chain, would result in lack of stabilization of the transition state leading to low catalytic rates (11). In addition, Lys 949 and Glu 950 of L6$_c$, whose positions are stabilized by interactions with Lys 935, make multiple polar contacts with the *ras* switch 1 domain.

Uniquely in the GAP complex, Lys 88 of p21, that does not occur in either switch 1 or 2 domains and does not interact with the *raf* RBD or with SOS, interacts with Thr 791 and Thr 792 of the GAP finger loop region (11). On the other hand, the *ras*-p21 domain involving residues 96-110, that interacts with SOS (12) (Section 4.2.4 above) and blocks oncogenic *ras*-p21-JNK/*jun* interactions (7, 45, 46) (Section 4.1.4 above), does not interact with any GAP residues (11).

Since substitutions in *ras* and GAP for such critical amino acid residues as Gln 61 in p21 and Arg 789 in GAP decrease GTPase activity, this decreased GTPase activity may result in prolonged *ras* proliferation signaling. Consistent with this hypothesis is the finding that mutation of Lys 1423 of the neurofibromin protein, a member of the GAP family, which is equivalent, by homology, to Lys 935 in GAP, causes severe decrease in GTPase activity and tumor formation (63).

On the other hand, as noted in the Introduction, there is considerable evidence that GAP may function as a target of *ras*-p21 on its signal transduction pathway in a manner that may not depend on its GTPase-enhancing ability. *ras*-bound GAP is known to stimulate activation of JNK (64), and may be important in regulation of apoptotic signaling through downstream regulation of caspase activity (65). Therefore GAP may well function as a target of *ras*-p21 in mitogenic signaling. Thus we have analyzed the effects of oncogenic amino acid substitutions in *ras*-p21 on the average structure of the *ras*-p21-GAP complex.

4.2.5.1. Results of Molecular Dynamics Calculations on *ras*-p21-GAP Complexes

Structural Changes in ras-p21. Superposition of the average three-dimensional structures of oncogenic and wild-type *ras*-p21, from the molecular dynamics calculations, is shown in Figure 9B. This superposition reveals that they have the same overall chain fold, but there are domains of both complexes that change conformation (66). Some domains of *ras*-p21 undergo structural changes, mainly at residues 66-77 containing the carboxyl terminal half of the switch 2 domain, in the 96-110 domain and in the domain containing residues 130-140. Smaller changes occur in the switch 1 domain (residues 32-47), around residue 88 and the 115-126 effector domain (66).

It is interesting that the 96-110 domain, that is not involved in binding to GAP, undergoes a structural change. This domain interacts with SOS and is the one that is involved with activation of JNK by oncogenic *ras*-p21 as noted in Sections 4.1.1 and 4.1.2 above. Since GAP may be involved in *ras*-p21 activation of JNK (64), one mechanism of this activation may be through stabilization of the binding conformation of this *ras*-p21 domain by GAP binding.

As has been found in the *ras*-p21-SOS complexes, residues 130-140 also undergo considerable changes in conformation in *ras*-p21-GAP complexes. This domain of *ras*-p21 is not known to interact with any known *ras*-p21 target.

In contrast, the *ras*-p21 switch 1 domain and

especially residues 66-77 of the switch 2 domain all interact strongly with GAP and adopt different positions when the average structures for the two complexes are superimposed. Such changes should lead to corresponding changes in the structures of GAP.

Changes in GAP Structure. We have found that five domains of GAP undergo major changes in conformation when the two average structures are superimposed: 819-827, 832-845, 917-926, 943-953 and 1003-1020 (66). Of these, only the 943-953 segment, that contains the critical Lys 949 and Glu 950 residues, interacts directly with *ras*-p21. The other three sequences do not interact with *ras*-p21 and occur on the surface of the protein where they are in a good position to interact with target proteins.

Comparison of Contacts in the Average Structures with those in the X-ray Structure. Many of the contacts between Val 12- and wild-type *ras*-p21 and GAP in their average structures are similar to those observed in the x-ray crystal structure (11). On the other hand, some contacts that exist in the energy-minimized x-ray structure are replaced by nearby amino acid residues in both average structures. For example, Gln 25 of *ras*-p21 interacts with Lys 949 from GAP in the x-ray structure while in the average structures, the interaction with Gln 25 is replaced with Glu 945 from GAP; Ile 36 in the switch 1 domain makes hydrophobic contacts with Leu 902 in GAP in the x-ray structure while it makes hydrophobic contacts with nearby GAP residue Leu 910; similarly, Ser 39 of the switch 1 domain interacts with Glu 950 in the x-ray structure while it interacts more closely with nearby residue Lys 949 in the average structures (66). These results suggest that there are "fluid" interactions between the two proteins in the complex such that contacts between them can alternate between different residues (66).

Differences in GAP Contacts in the Two Average Structures. There are two major differences in contacts in the two average structures between *ras*-p21 and GAP. First, the switch 2 domain residues 66-77 of oncogenic *ras*-p21 make contacts with GAP while these residues in the wild-type *ras*-p21 make no close contacts with GAP; second, a putative catalytically important interaction between the carboxamido NH_2 of Gln 61 and the backbone carbonyl oxygen of Arg 789 in the x-ray structure exists only in the wild-type complex. These results suggest the possibility that oncogenic *ras*-p21 binds tightly to GAP in a non-catalytic binding mode while wild-type *ras*-p21 may have fewer interactions with GAP but forms a complex that can undergo catalysis (66).

4.2.5.2. GAP Domain Peptides Inhibit *ras*-p21 Signaling (67)

We have synthesized and microinjected both *ras*-p21 (residues 66-77 and 122-138) and the five GAP domain peptides from this study into oocytes either co-injected with oncogenic *ras*-p21 or incubated with insulin. As shown in entries 5 and 6 and 11 and 12, the two new *ras*-p21 peptides, 66-77 and 122-138, inhibit both oncogenic *ras*-p21- and insulin-induced oocyte maturation but more strongly block oncogenic *ras*-p21 (67). The *ras*-p21 66-77 peptide corresponds to about half of the switch 2 domain which is involved in interactions of *ras*-p21 with SOS and, as noted in Section 4.1 above, is important in transducing structural changes from amino to carboxyl terminal domains of *ras*-p21 itself (37). Thus its ability to inhibit both oncogenic *ras*-p21 and insulin-induced maturation is not surprising. On the other hand, it blocks oncogenic *ras*-p21 to a greater extent (compare entry 5 to entry 6 in Figure 4). One possible explanation for this result is that this peptide may block the unique contacts made by the 66-77 segment of oncogenic *ras*-p21 with GAP.

Importantly, as shown in Figure 4, the three GAP peptides, 832-845 (entries 21 and 22), 943-953 (containing the two critical contact residues Lys 949 and Glu 950, entries 25 and 26) and 1003-1021 (entries 27 and 28), which almost completely blocks insulin-induced maturation (66), appear to inhibit insulin-induced maturation more strongly than they inhibit maturation induced by oncogenic *ras*-p21, suggesting that these domains of GAP may play an important role on pathways more important for activated wild-type *ras*-p21. On the other hand, GAP domain peptides 819-827 (entries 19 and 20) and 917-926 (entries 23 and 24) inhibit both oncogenic *ras*-p21- and insulin-induced maturation to about the same extent. Especially for these latter two peptides, as discussed in Section 4.2.2 above, the possibility exists that, irrespective of their positions on the surface of GAP, each domain is critical to both pathways or that each domain covers other critical domains that are required for activation of common downstream targets.

All seven peptides, designed from the *ras*-p21-GAP structures, appear to inhibit pathways specific to *ras*-p21 proteins since none of these peptides was found to inhibit progesterone-induced maturation (67). However, since, as with SOS, GAP does not induce oocyte maturation (H.-F. Kung, personal communication), the specificity of inhibition of these peptides for GAP on the *ras*-induced signal transduction pathways has not been established. Further studies, as with the SOS peptides, are needed to establish the site(s) of inhibition of these peptides.

4.2.5.3. Conclusions

As found for the *ras*-p21 complexes with the RBD of *raf* and SOS, conformational analysis of complexes of *ras*-p21 with GAP reveal effector domains of GAP and two other effector domains of *ras*-p21 itself. Our results suggest that GAP may also be involved in *ras*-p21-promoted signal transduction in addition to its functioning as a negative regulatory protein on *ras*-p21 activity. Surprisingly, several peptide domains of GAP appear to be involved more prominently with signal transduction by activated wild-type *ras*-p21 and may be useful in the identification of important targets of this protein.

4.3. Dynamics Calculations on GST-pi, a Specific JNK-*jun* Inhibitor

As noted in Section 4.1.4 above, we have found that GST-pi is a potent and specific inhibitor of the JNK-induced phosphorylation of *jun* (25, 26, 48). GST-pi is a

known xenobiotic-metabolizing enzyme that conjugates foreign compounds with electrophilic centers to thio ethers of glutathione. Mutant GST-pi, which is catalytically inactive, nonetheless inhibits JNK activation of *jun* (25, 26). Thus the ability of GST to inhibit JNK-*jun* does not correlate with its enzymatic activity (25, 26).

On the other hand, the binding of certain GST-pi inhibitors, such as glutathione-S-sulfonate and S-n-hexyl-glutathione, also block the ability of this enzyme to interfere with JNK-induced activation of *jun* (25, 26). This result suggests that the inhibitors may change the conformation of GST-pi, preventing domains of this enzyme from interacting with the complex (26).

To determine the location and structures of these putative domains, we have performed molecular dynamics calculations on the energy-minimized x-ray structures of free GST-pi and GST-pi bound to glutathione-S-sulfonate to superimpose the average structures of these complexes (26). These calculations were not on complexes of *ras*-p21 but are rather on a vitally important protein that blocks the oncogenic form of this protein. An important objective was to determine if GST-pi effector peptides exist that can mimic the effect of the whole protein and which can be used to inhibit oncogenic *ras*-p21 selectively.

In the superposition of the two average structures, we have found that four domains involving residues 34-50, 99-121, 165-182 (with two overlapping sub-domains 165-175 and 169-182) and 194-201. Of these domains, the 35-50 segment is involved in making contacts with GST substrates (26).

We have synthesized peptides corresponding to these domains and assayed them for their abilities to affect the activation of *jun* by JNK (26, 48). In these experiments, bead-bound JNK-*jun* complexes were incubated with GST-pi alone or with GST-pi plus one of the peptides, and *jun* phosphorylation was measured by either blotting for phospho-*jun* or by determining *jun* ^{32}P incorporation from ATP^{32}. The same experiments were also performed in the absence of GST-pi (48).

We have found that the 99-121 and 194-201 domain peptides strongly inhibit the ability of GST-pi to block *jun* phosphorylation, which we have found is due to its diminished binding to the JNK-*jun* complex but do not, by themselves inhibit JNK-induced phosphorylation of *jun*, while peptides corresponding to residues 34-50 and 165-182 do not inhibit GST binding but, except for the 165-175 subdomain peptide, strongly inhibit *jun* phosphorylation (48). The control X13 peptide had no effect on either binding or phosphorylation. These inhibitory effects on binding or phosphorylation appear to be selective for the JNK-*jun* system since the 34-50 peptide has no effect on other kinases such as casein kinase and MAP kinase systems (48).

To test the effects of GST domain peptides in cells, as with the two *ras*-p21 peptides, we synthesized three of these domain peptides, 34-50, 165-175 and 194-201, with the penetratin sequence attached to their carboxyl terminal ends, enabling transmembrane transport into cells. We then incubated these peptides with human astrocytes in which JNK was activated with anisomycin, a known JNK activator (48). We find that the 34-50-penetratin peptide strongly inhibits intracellular *jun* phosphorylation while the 194-201-penetratin peptide has no effect; the 165-175-penetratin peptide has a weak effect on this process. Thus the effects in cells parallels those in the cell-free system (48).

These studies suggest that the 35-50 GST-pi domain peptide inhibits *jun* phosphorylation by JNK but does not interfere with the interaction of preformed GST-JNK-*jun* complexes. Thus it does not remove GST-pi inhibition of the JNK-*jun* system but will inhibit JNK-induced phosphorylation of *jun* in complexes unbound to GST-pi. This peptide would therefore appear to be an ideal inhibitor of oncogenic *ras*-p21 signaling since it would mimic the selective inhibitory effects of the entire GST-pi protein on oncogenic *ras*-p21.

We have recently co-injected this peptide into oocytes with oncogenic *ras*-p21 and into oocytes incubated with insulin and have found that it strongly inhibits oncogenic *ras*-p21-induced oocyte maturation while it has only minimal effects on insulin-induced maturation (68) as shown in entries 49 and 50 in Figure 4. Thus this peptide appears to have potential as another agent that can block *ras*-induced cancers without affecting the growth of normal cells.

5. CONCLUSIONS

Our approach of employing conformational energy calculations to computing the average structures of oncogenic and wild-type *ras*-p21 and of these proteins bound to target and regulatory proteins has resulted in our identifying peptide effector domains of these proteins. All of the peptides corresponding to these domains have been found to have inhibitory activity against *ras*-dependent mitogenic signal transduction as summarized in Figure 4, using the oocyte system. That these peptides inhibit signaling events specifically on the *ras* pathway is suggested by our findings that they all inhibit oncogenic *ras*-p21- and/or wild-type *ras*-p21-dependent insulin-induced oocyte maturation but not *ras*-independent progesterone-induced oocyte maturation.

Importantly, while several of these domains have been identified as having functional importance in molecular and cell biological experiments such as the switch 1 and switch 2 domains of *ras*-p21 and the 62-76 domain of the RBD of *raf*, most of these domains were identified from the computational work. Several peptides corresponding to these domains preferentially inhibit mitogenic signaling of oncogenic *ras*-p21 while they only minimally affect insulin-activated wild-type *ras*-p21 in the oocyte system. These peptides include *ras*-p21 residues 35-47 (entries 3 and 4 in Figure 4), 96-110 (entries 7 and 8 in Figure 4), 115-126 (entries 9 and 10 in Figure 4) and, to a lesser extent, 122-138 (entries 11 and 12 in Figure 4); *raf* RBD residues 97-110 (entries 15 and 16 in Figure 4); and SOS residues 980-989 (entries 43 and

44 in Figure 4) and 994-1004 (entries 35 and 36 in Figure 4). Also, although not a direct target of *ras*-p21, the GST 34-50 peptide, that blocks JNK-induced phosphorylation of *jun*, a process critical to the oncogenic *ras*-p21 pathway, selectively blocks oncogenic *ras*-p21 (entries 49 and 50 in Figure 4).

Our finding that these peptides preferentially block oncogenic *ras*-p21 supports the conclusion that, despite only a single amino acid substitution between oncogenic and wild-type *ras*-p21, the two proteins induce mitogenesis by divergent pathways. This seems to hold in two ways. First, there appear to be unique targets on the oncogenic *ras*-p21 pathway, in particular, direct activation of JNK/*jun* (interfered with by the *ras*-p21 96-110 and 115-126 peptides), that are not required on the activated wild-type *ras*-p21 pathway. Second, each protein appears to interact with common target proteins, such as *raf*, differently. For example, our molecular dynamics calculations show that, while both *ras* proteins bind to the RBD of *raf*, residues 44-47 of the switch 1 domain interact differently with this target. The consequence of these different interactions appears to be that the *ras*-p21 35-47 peptide preferentially blocks the interaction of oncogenic *ras*-p21 with the RBD allowing for normal signal transduction.

Conversely, several peptides, mainly from GAP, inhibit insulin-induced oocyte maturation to a significantly greater extent than they inhibit oncogenic *ras*-p21. These include GAP peptides 832-845, 943-953 and 1003-1021. Peptides that preferentially inhibit oncogenic *ras*-p21- or insulin-induced oocyte maturation are valuable as probes for determining crucial steps on each signal transduction pathway.

Since we find that domain peptides from GAP and SOS inhibit oocyte maturation induced by oncogenic *ras*-p21 and/or by insulin, it is plausible that these two proteins may be involved in *ras*-p21-activated signal transduction, in addition to their regulatory functions. As we noted in Sections 4.2.4.3 and 4.2.5.2 above, since we have not established functional assays for either of these two proteins, it is possible that the inhibitory peptides block *ras*-dependent signaling at signal transduction steps that do not involve these two proteins. On the other hand, five GAP peptides and eight SOS peptides, each containing a minimum of 10 and a maximum of 22 residues from each domain, all inhibit *ras*-induced oocyte maturation while negative control peptides such as the *raf* 84-92 and SOS 809-815 peptides have no effect on either oncogenic *ras*-p21- or insulin-induced oocyte maturation. It seems less likely that all 13 of these domain peptides would inhibit only at steps that do not involve either of these two proteins.

An important practical application of our discovery of domain peptides that block oncogenic *ras*-p21 selectively in oocytes, has been our introducing them into *ras*-induced cancer cells by attaching them to the penetratin sequence as potential anti-cancer agents. Since neither of these peptides affects insulin-induced oocyte maturation, we reasoned that in *ras*-transformed mammalian cancer cells, these peptides might block abnormal proliferation signals from oncogenic *ras*-p21 while leaving normal growth signals intact.

Thus far we find that two of these peptides, *ras*-p21 35-47, that blocks oncogenic *ras*-p21 at the level of *raf* and 96-110, that blocks direct activation of JNK by oncogenic *ras*-p21, both block the growth of *ras*-transformed TUC-3 pancreatic cancer cells. Significantly, these peptides do not induce cell death but rather induce phenotypic reversion of the cells to the untransformed phenotype, supporting our supposition that these peptides would block only abnormal proliferation signals.

These results also suggest that these peptides and, possibly the other oncogenic-*ras*-specific peptides, may be effective agents in treating *ras*-induced human cancers.

6. ACKNOWLEDGEMENTS

This work was supported in part by NIH Grant CA 42500 (MRP), a VA Merit Review Grant (MRP), and a grant from the Lustgarten Foundation for Pancreatic Cancer Research (MRP).

7. REFERENCES

1. Pincus, M.R., P.W. Brandt-Rauf, W. Koslosky and W. Appruzzese: In: Cell Biology and Early Tumor Detection (Chapter 64). Ed.: Henry, J.B., *Clinical Diagnosis and Management by Laboratory Methods*, Nineteenth Edition, W.B. Saunders, Philadelphia, 1344-1354 (2001)

2. Haffner, R. and M. Oren: Biochemical properties and biological effects of p53. *Curr Opin Genet Dev* 5, 84-90 (1995)

3. Stacey, D.W. and H.-F. Kung,: Transformation of NIH 3T3 cells by microinjection of Ha-ras p21 protein. *Nature* (London), 310, 508-511 (1984)

4. Barbacid, M. *ras* Genes: *Ann Rev Biochem* 56, 779-827 (1987)

5. Birchmeier, C., D. Broek, and M. Wigler: *ras* proteins can induce meiosis in *Xenopus* oocytes. *Cell* 43, 615-621 (1985)

6. Deshpande, A.K. and H.-F. Kung: Insulin induction of *Xenopus laevis* oocyte maturation is inhibited by monoclonal antibody against p21 *ras* proteins. *Mol Cell Biol* 7, 1285-1288 (1987)

7. Pincus, M.R., P.W. Brandt-Rauf, J. Michl and F.K. Friedman: *ras*-p21-Induced Cell Transformation: Unique Signal Transduction Pathways And Implications for the Design of New Chemotherapeutic Agents. *Cancer Invest* 18, 39-50 (2000)

8. Manne, V., C.S. Ricca, J.G. Brown, A.V. Tuomari, N. Yan, D. Patel, R. Schmidt, M.J. Lynch, C.P. Closek Jr., J.M. Carboni, S. Robinson, E.M. Gordon, M. Barbacid, B.R. Seizinger and S.A. Biller: *ras* farnesylation as a target

for nnovel antitumor agents: Potent and selective farnesyl diphosphate analogue inhibitors of farnesyltransferase. *Drug Dev Res* 34, 121-137 (1995)

9. Karin, M.: Regulation of activity by mitogen activated protein kinases. *J Biol Chem* 270, 16483-16486 (1995)

10. Nassar, N., G. Horn, C. Herrmann, A. Scherer, F. McCormick and A. Wittinghofer: The 2.2 Å crystal structure of the ras-binding domain of the serine/threonine kinase c-raf-1 in complex with rap-1a and a GTP analogue. *Nature* (London) 375, 554-560 (1995)

11. Scheffzek, K., M.R. Ahmadian, W. Kabsch, L. Weismuller, F. Lautwein-Schmitz, and A. Wittinghofer: The *ras-ras* GAP complex: structural basis for GTPase activation and its loss in oncogenic ras mutants. *Science* 227, 333-338 (1997)

12. Boriak-Sjodin, P.A., S.M. Margarit, D. Bar-Sagi and J. Kuriyan: The structural basis of the activation of ras by SOS. *Nature* (London) 394, 337-343 (1998)

13. Rodriguez-Viciana, P., P.H. Warne, R. Dhand, B. Vanhaesebroeck, I. Gout, M.J. Fry, M.D. Waterfield and J. Downward: Phosphatidylinositol-3-OH kinase as a direct target of Ras. *Nature* (London) 370, 527-532 (1994)

14. Krengel, U., L. Schlichting, A. Scherer, R. Schumann, M. Frech, J. John, W. Kabsch, E.F. Pai and A. Wittinghofer: Three-dimensional structures of H-*ras* p21 mutants: Molecular basis for their ability to function as signal switch molecules. *Cell* 62, 539-548 (1990)

15. Der, C.J., T. Finkel and G.M. Cooper: Biological and biochemical properties of human *ras*h genes mutated at codon 61. *Cell* 44, 167-176 (1986)

16. Clanton, D.J., Y. Lu, D.G. Blair and T.Y. Shih: Structural significance of the GTP-binding domain of *ras* p21 studied by site-directed mutagenesis. *Mol Cell Biol* 7, 3092-3097 (1987)

17. Moodie, S.A., B.M. Willumsen, M.J. Weber and A. Wolfman: Complexes of ras-GTP with raf-1 and mitogen-activated protein kinase. *Science* 260, 1658-1661 (1993)

18. Scheraga, H.A.: Predicting Three-Dimensional Structures of Oligopeptides. *Reviews in Comput Chem* III, 73-142 (1992)

19. Post, C.B., B.R. Brooks, M. Karplus, C.M. Dobson, P.J. Artymiuk, J.C. Cheetham and D.C. Phillips: Molecular dynamics simulations of native and substrate-bound lysozyme. A study of the average structures and atomic fluctuations. *J Mol Biol* 190, 455-479 (1986)

20. Weiner, S.J., P.A. Kollman, D.A. Case, V.C. Singh, C. Ghio, G. Alagona, S. Profeta and P.K. Weiner: A new force field for molecular simulations of nucleic acids and proteins. *J Amer Chem Soc* 106, 765-784 (1986)

21. Dauber-Osguthorpe, P., V.A. Roberts, D.J. Osguthorpe, J. Wolff, M. Genest and A.T. Hagler: Structure and energetics of ligand binding to proteins: E. coli dihydrofolate reductase-trimethoprim, a drug-receptor system. *Proteins: Structure, Function Genet* 4, 31-47 (1988)

22. Ripol, D. and H.A. Scheraga: On the multiple-minima problem in the conformational analysis of polypeptides. II. An Electrostatically-Driven Monte Carlo method. Tests on poly-(L-Alanine). *Biopolymers* 27, 1283-1303 (1988)

23. Piela, L. and H.A. Scheraga: On the multiple-minimum problem in the conformational analysis of polypeptides. I. Backbone degrees of freedom for a perturbed alpha-helix. *Biopolymers* 26, S33-S58 (1987)

24. Nemethy, G., M.S. Pottle and H.A. Scheraga: Energy parameters in polypeptides. 9. Updating of geometrical parameters, nonbonded interactions and hydrogen bond interactions for the naturally occurring amino acids. *J Phys Chem* 87, 1883-1887 (1983)

25. Adler, V., Z. Yin, S. Fuchs, M. Benezra, L. Rosario, K. Tew, M.R. Pincus, M. Sardana, C. Henderson, C.R.Wolf, R. Davis and Z. Ronai,: GSTpi-a regulator of JNK signaling. *EMBO J* 18, 1321-1334 (1999)

26. Monaco, R., F.K. Friedman, M.J. Hyde, J.M. Chen, S. Manolatus, V. Adler, Z. Ronai, W. Koslosky and M.R. Pincus: Identification of a glutathione-s-transferase effector domain for inhibition of *jun* kinase, by molecular dynamics. *J Protein Chem* 18, 859-866 (2000)

27. Garcia-Saez, I., A. Parraga, M.F. Phillips, T.J. Mantle and M. Coll: Molecular structure at 1.8 Å of mouse liver class pi glutathione-s-transferase complexed with s-(p-nitrobenzyl)glutathione and other inhibitors. *J Mol Biol* 237, 298-314 (1994)

28. Dykes, D.C., P.W. Brandt-Rauf, S.M. Luster, F.K. Friedman and M.R. Pincus: Activated conformations of the ras-gene-encoded p21 protein. 2. Comparison of the computed and high-resolution x-ray crystallographic structures of Gly 12-p21. *J Biomol Struct Dynamics* 10, 905-918 (1993)

29. Monaco, R., J.M. Chen, D.L. Chung, P.W. Brandt-Rauf and M.R. Pincus: Comparison of the Computed Three-Dimensional Structures of Oncogenic Forms of the ras-Gene-Encoded p21 Protein with the Structure of the Normal (Non-Transforming) Wild-Type Protein. *J Protein Chem* 14, 457-466 (1995)

30. Monaco, R., J.M. Chen, F.K. Friedman, P.W. Brandt-Rauf and M.R. Pincus: Structural effects of the binding of GTP to the wild-type and oncogenic forms of the ras-gene-encoded p21 proteins. *J Protein Chem* 14, 721-730 (1995)

31. Vasquez, M., G. Nemethy and H.A. Scheraga: Computed conformational states of the 20 naturally occurring amino acid residues and of the prototype residue, alpha-amino butyric acid. *Macromolecules* 16, 1043-1049 (1983)

32. Miura, K., Y. Inouye, H. Nakamori, S. Iwai, E. Ohtsuka,

M. Ikehara, S. Noguchi, and S. Nishimura: Synthesis and expression of a synthetic gene for the activated human c-Ha-*ras* protein. *Jpn J Cancer Res* (Gann) 77, 45-51 (1986)

33. Kovac, C., L. Chie, J. Morin, F.K. Friedman, R. Robinson, D.L. Chung, M. Kanovsky. J. Flom, P.W. Brandt-Rauf, Z. Yamaizumi, J. Michl and M.R. Pincus: Plasmid expression of a peptide that selectively blocks oncogenic *ras*-p21-induced oocyte maturation. *Cancer Chemother Pharmacol* 45, 441-449 (2000)

34. Chie, L., S. Amar, H.-F. Kung, M.C.M. Lin, H. Chen, D. Chung, V. Adler, Z. Ronai, F.K. Friedman, R.C. Robinson, C. Kovac, P.W. Brandt-Rauf, Z. Yamaizumi, J. Michl, and M.R. Pincus: Induction of oocyte maturation by *jun*-n-terminal kinase (jnk) on the oncogenic *ras*-p21 pathway is dependent on the *raf*-mek signal transduction pathway. *Cancer Chemother Pharmacol* 45, 441-449 (2000)

35. Kanovsky, M., J. Michl, G. Botzolaki, J. Morin, C. Kovac, D. Chung, F.K. Friedman and M.R. Pincus: Peptides, designed from molecular modeling studies of the *ras*-p21 protein, induce phenotypic reversion of a pancreatic carcinoma cell line but have no effect on normal pancreatic acinar cell growth. *Cancer Chemother Pharmacol* 52, 202-208 (2003)

36. Kanovsky, M., A. Raffo, L. Drew, R. Rosal, T. Do, F.K. Friedman, P. Rubinstein, I. Visser, R. Robinson, P.W. Brandt-Rauf, J. Michl, R.L. Fine and M.R. Pincus: Peptides from the amino terminal mdm-2 binding domain of p53, designed from conformational analysis, are selectively cytotoxic to transformed cells. *Proc Natl Acad Sci USA* 98, 12438-12443 (2001)

37. Liwo, A., K.D. Gibson, H.A. Scheraga, P.W. Brandt-Rauf, R. Monacyo, and M.R. Pincus: Comparison of the low energy conformations of an oncogenic and a non-oncogenic p21 protein, neither of which binds GDP or GTP. *J Protein Chem* 13, 237-251 (1994)

38. de Vos, A.M., L. Tong, M.V. Milburn, P.M. Matias, J. Jancarik, S. Noguchi, S. Nishimura, K. Miura, E. Ohtsuka and S.-H. Kim: Three-dimensional structure of an oncogene-protein: catalytic domain of human c-H-ras p21. *Science* 239, 888-893 (1988)

39. Brandt-Rauf, P.W., R.P. Carty, J.M. Chen, G. Lee, S. Rackovsky and M.R. Pincus: The Structure of the Carboxyl Terminus of the p21 Protein. Structural Relationship to the Nucleotide Binding/Transforming Regions of the Protein. *J Protein Chem* 9, 137-142 (1990)

40. Chung, D.L., P.W. Brandt-Rauf, R.B. Murphy, S. Nishimura, Z. Yamaizumi, I.B. Weinstein and M.R. Pincus: A peptide from the gap-binding domain of the ras-p21 protein and azatyrosine block ras-induced maturation of xenopus oocytes. *Anticancer Res* 11, 1373-1378 (1991)

41. Chung, D.L., P.W. Brandt-Rauf, I.B. Weinstein, S. Nishimura, Z. Yamaizumi, R.B. Murphy and M.R. Pincus: Evidence that the *ras* oncogene-encoded p21 protein induces oocyte maturation via activation of protein kinase C. *Proc Natl Acad Sci USA* 89, 1993-1996 (1992)

42. Chung, D.L., A. Joran, F.K. Friedman, R.R. Robinson, P.W. Brandt-Rauf, I.B. Weinstein, Z.A. Ronai, L. Baskin, D.C. Dykes, R.B. Murphy, S. Nishimura, Z. Yamaizumi and M.R. Pincus: Evidence that oocyte maturation induced by an oncogenic ras p21 protein and insulin is mediated by overlapping yet distinct mechanisms. *Exp Cell Res* 203, 329-335 (1992)

43. Lee, L., Z.A. Ronai, M.R. Pincus, P.W. Brandt-Rauf, R.B. Murphy, T.M. Delohery, S. Nishimura, Z. Yamaizumi and I.B. Weinstein: Identification of an intracellular protein which specifically interacts with photoaffinity-labelled oncogenic p21 protein. *Proc Natl Acad Sci USA* 86, 8678-8682 (1989)

44. Baskin, L., J. Haspel, K. O'Driscoll, Z. Ronai, F. Friedman, P.W. Brandt-Rauf, D. Chung, I.B. Weinstein, S. Nishimura, Z. Yamaizumi, G. Singh, D. Dykes, R. Murphy and M.R. Pincus: A 43kDa Protein (p43) that Interacts with the ras-Oncogene-Encoded p21 Protein Strongly Induces Maturation of Oocytes. *Med Sci Res* 20, 813-815 (1992)

45. Adler, V., M.R. Pincus, P.W. Brandt-Rauf and M.R. Pincus: Complexes of ras-p21 with jun-N-Kinase and c-jun proteins. *Proc Natl Acad Sci USA* 92, 10585-10589 (1995)

46. Adler, V., M.R. Pincus, A. Polatskaya, X. Montano, F.K. Friedman and Z. Ronai: Activation of c-*jun* NH_2 kinase by uv irradiation is dependent on $p21^{ras}$. *J Biol Chem* 271, 23304-23309 (1996)

47. Ranginwale, M., S. Smith, J. Flom, L. Chie, M. Kanovsky, D. Chung, F.K. Friedman, R.C. Robinson, P.W. Brandt-Rauf, Z. Yamaizumi, J. Michl, and M.R. Pincus: Differences in patterns of activation of map kinases induced by oncogenic ras-p21 and insulin in oocytes. *Exp Cell Res* 269, 162-169 (2001)

48. Adler, V. and M.R. Pincus: Effector peptides from glutathione-s-transferase-pi affect the activation of *jun* by *jun*-N-terminal kinase. *Ann Clin Lab Sci* 34, 35-46 (2004)

49. Villafania, A., K. Anwar, S. Amar, D. Chung, V. Adler, Z. Ronai, P.W. Brandt-Rauf, Z. Yamaizumi, H.-F. Kung and M.R. Pincus: Glutathione-S-transferase as a selective inhibitor of oncogenic *ras*-p21-induced mitogenic signaling through blockade of activation of *jun* by *jun*-n-terminal kinase. *Ann Clin Lab Sci* 30, 61-68 (1999)

50. Amar, S., A. Glozman, D.L. Chung, V. Alder, Z. Ronai, F.K. Friedman, R. Robinson, P.W. Brandt-Rauf, Z. Yamaizumi and M.R. Pincus: Selective inhibition of oncogenic *ras*-p21 *in vivo* by agents that block its interaction with *jun*-N-terminal-kinase (JNK) and *jun* proteins. Implications for the design of selective chemotherapeutic agents. *Cancer Chemother and Pharmacol* 41, 79-85 (1997)

51. Chie, L., J.M. Chen, F.K. Friedman, D.L. Chung, S. Amar, J. Michl, Z. Yamaizumi, P.W. Brandt-Rauf and M.R. Pincus: Identification of the site of inhibition of oncogenic *ras*-p21-induced signal transduction by a peptide from a *ras* effector

domain. *J Protein Chem* 18, 881-884 (2000)

52. Chie, L., F.K. Friedman, H.-F. Kung, M.C.M. Lim, D.L. Chung and M.R. Pincus: Identification of the site of inhibition of mitogenic signaling by oncogenic *ras*-p21 by a *ras* effector peptide. *J Protein Chem* 21, 367-369 (2002)

53. Clark, J., J.K. Drugan, R.S. Terrell, C. Bradham, C.J. Der, R.M. Bell and S. Campbell: Peptides containing a consensus ras binding sequence from raf-1 and the gtpase activating protein nf1 inhibit ras function. *Proc Natl Acad Sci USA* 93, 1577-1581 (1996)

54. White, M.A., C. Nicolette, A. Minden, A. Polverino, L. van Aelst, M. Karin and M. Wigler: Multiple ras functions can contribute to mammalian cell transformation *Cell* 80, 533-541 (1995)

55. Chen, J.M., R. Monaco, S. Manolatos, P.W. Brandt-Rauf, F.K. Friedman and M.R. Pincus: Molecular dynamics on complexes of *ras*-p21 and its inhibitor protein, rap-1a, bound to the *ras*-binding domain of the *raf*-p74 protein. Identification of effector domains in the *raf* protein. *J Protein Chem* 16, 631-635 (1997)

56. Chen, J.M., K. Rijwani, F.K. Friedman, M.J. Hyde and M.R. Pincus: Identification, using molecular dynamics, of an effector domain of the *ras*-binding domain of the *raf*-p74 protein that is uniquely involved in oncogenic *ras*-p21 signaling. *J Protein Chem* 7, 543-549 (2000)

57. Chung, D., S. Amar, A. Glozman, J.M. Chen, F.K. Friedman, R. Robinson, R. Monaco, P.W. Brandt-Rauf, Z. Yamaizumi and M.R. Pincus: Inhibition of oncogenic and activated wild-type ras-p21 protein-induced oocyte maturation by peptides from the *ras* binding domain of the *raf*-p74 protein, identified from molecular dynamics calculations. *J Protein Chem* 16, 619-629 (1997)

58. Chen, J.M., F.K. Friedman, M.J. Hyde, R. Monaco and M.R. Pincus: Molecular dynamics analysis of the structures of *ras*-guanine nucleotide exchange protein (SOS) bound to wild-type and oncogenic-*ras*-p21. Identification of effector domains of SOS. *J Protein Chem* 18, 867-874 (2000)

59. Duncan, T., J.M. Chen, F.K. Friedman, M. Hyde and M.R. Pincus: Comparison of molecular dynamics averaged structures for complexes of normal and oncogenic *ras*-p21 with SOS nucleotide exchange protein, containing computed conformations for three crystallographically undefined domains, suggests a potential role of these domains in *ras* signaling. *The Protein J* 23, 217-228 (2004)

60. Chie, L., J.M. Chen, F.K. Friedman, D.L. Chung, S. Amar, J. Michl, Z. Yamiazumi and M.R. Pincus: Inhibition of oncogenic and activated wild-type *ras*-p21 protein-induced peptides from the guanine-nucleotide exchange protein, SOS, identified from molecular dynamics calculations. Selective inhibition of oncogenic *ras*-p21. *J Protein Chem* 18, 875-879 (2000)

61. Chie, L., F.K. Friedman, T. Duncan, J.M. Chen, D.L. Chung and M.R. Pincus: Loop domain peptides from the sos *ras*-guanine nucleotide exchange protein, identified from molecular dynamics calculations, strongly inhibit *ras* signaling. *The Protein J* 18, 229-234 (2004)

62. Crennell, S., E. Garman, G. Laver, E. Vimr and G. Taylor: Crystal structure of *Vibrio cholerae* meuraminidase reveals dual lectin-like domains in addition to the catalytic domain. *Structure* 2, 535-544 (1994)

63. Poullet, P., B. Lin, K. Esson and F. Tamanoi: Functional significance of lysine 1423 of neurofibromin and characterization of a second site suppressor which rescues mutations at this residue and suppresses ras2val-19-activated phenotypes. *Mol Cell Biol* 14, 815-821 (1994)

64. Clark, G.J., J.K. Westwick and C.J. Der: p120 GAP modulates *ras* activation of *jun* kinases and transformation. *J Biol Chem* 272, 1677-1681 (1997)

65. Yang, J.-Y. and C. Widmann: Anti-apoptotic signaling generated by caspase-induced cleavage of RasGAP. *Mol Cell Biol* 21, 5346-5358 (2001)

66. Chen, J.M., F.K. Friedman, P.W. Brandt-Rauf and M.R. Pincus: Comparison of the average structures, from molecular dynamics, of complexes of GTPase activating protein (GAP) with oncogenic and wild-type *ras*-p21: Identification of potential effector domains. *J Protein Chem* 21, 349-359 (2002)

67. Friedman, F.K., L. Chie, D.L. Chung, R. Robinson, P.W. Brandt-Rauf, Z. Yamaizumi and M.R. Pincus: Inhibition of *ras*-induced oocyte maturation by peptides from *ras*-p21 and gtpase activating protein (gap) identified as being effector domains from molecular dynamics calculations. *J Protein Chem* 21, 361-366 (2002)

68. Chie, L., F.K. Friedman, D.L. Chung and M.R. Pincus: An effector peptide from glutathione-s-transferase-pi strongly and selectively blocks mitotic signaling by oncogenic *ras*-p21. *The Protein J* 18, 235-238 (2004)

Note added in proof: Recently, a new set of ras-SOS structures have been determined (Margarit *et al* structural evidence for feedback activation by Ras-GTP of the Ras-specific nucleotide exchange factor SOS. *Cell* 112, 685-695 [2003]) in which it has been found that two ras molecule bind per mole of SOS, one in the site discussed in this paper, the other bound to non-hydrolysable GTP in another newly defined site. We are currently analyzing this structure.

Key Words: Conformational energy calculations, Electrostatically driven monte carlo calculations (EDMC), Molecular dynamics, Cell transformation, Oncogenic *ras*-p21, Insulin, Oocyte maturation, Effector domain peptides, Signal transduction pathway, Pancreatic cancer cell line, Anti-cancer peptides, Phenotypic reversion

Send correspondence to: Dr Matthew R. Pincus, Chief, Department of Pathology and Laboratory Medicine (113), New York Harbor VA Medical Center, 800 Poly Place, Brooklyn, NY 11209, Tel: 718-630-3688, Fax: 718-630-2960, E-mail: Matthew.Pincus2@med.va.gov